
AN ALL-REGIME, WELL-BALANCED, POSITIVE AND ENTROPY SATISFYING ONE-STEP FINITE VOLUME SCHEME FOR THE EULER'S EQUATIONS OF GAS DYNAMICS WITH GRAVITY

Rémi Bourgeois *
UVSQ, CNRS, CEA Saclay
Maison de la simulation
Université Paris-Saclay
remi.bourgeois@cea.fr

Pascal Tremblin
UVSQ, CNRS, CEA Saclay
Maison de la simulation
Université Paris-Saclay
pascal.tremblin@cea.fr

Samuel Kokh
DES/DANS/DM2S/STMF CEA Saclay
Université Paris-Saclay
samuel.kokh@cea.fr

Thomas Padioleau
UVSQ, CNRS, CEA Saclay
Maison de la simulation
Université Paris-Saclay
thomas.padioleau@cea.fr

ABSTRACT

In this paper, we propose a flux splitting finite volume method for the approximation of the Euler equations with source terms derived from a potential. The flux splitting strategy that we adopt here relies on a separate treatment of the terms related to pressure effects from the terms related to transport. We show that this approach can be recast into a relaxation approximation that shares similarities with the Lagrange-Projection method, so that the present flux splitting method can be viewed as an "unsplit Lagrange-Projection" algorithm. We perform a truncation analysis error in the low Mach regime that suggests a flux modification in order to preserve the accuracy of the method in this regime. We show that the resulting method is well-balanced in the sense that it preserves hydrostatic equilibrium profiles. Under a CFL condition, the numerical scheme is also positivity preserving for the mass and the internal energy and it also verifies a discrete entropy inequality. One-dimensional and two-dimensional numerical experiments show the ability of the method to deal with a wide range of Mach regime, shocks, rarefactions and to preserves hydrostatic equilibrium states.

1 Introduction

In this work we consider the approximation of the compressible Euler equations in the presence of source terms derived from a potential energy by means of a collocated finite volume method.

Our numerical method belongs to the category of flux splitting methods. Flux splitting methods have been used in many application contexts thanks to their ease of implementation that relies on building discrete evaluation of the fluxes (see for example [1, 2, 3, 4, 5]). These methods have been extensively developed for several decades (see for example [6, 7, 8, 9, 9, 10, 11, 12, 13, 14] and the references therein) yielding efficient simulation tools. Unfortunately, deriving theoretical results that ensure the good behavior of these methods is difficult which contrast with their good performance in practice.

Our aim is to propose a method that fulfills several key criteria without sacrificing ease of implementation: the method should be positivity preserving for both density and internal energy. In the low Mach regime, it should provide a uniform

*Corresponding author: Tel: +33 629 623 489
Preprint submitted to Journal of Computational Physics

truncation error with respect to the Mach number. The method should be conservative with respect to the pure convective effects. The discretization of the source term should be well-balanced (see for instance [15, 16, 17, 18, 19, 20] and the reference therein) in the sense that it should preserve null velocity stationary solutions of the system. We furthermore require the method to verify a discrete entropy inequality.

In order to achieve all these goals, we revisit a particular type of flux splitting that relies on separating acoustic and transport related fluxes [7, 21, 22]. Discretization techniques that also feature a separate treatment for the pressure and advection effects have been proposed for fractional step methods [23, 24, 25, 26, 27, 19, 28, 29]. By recasting the flux splitting evaluation into an averaging process we can adapt these methods to propose both a numerical flux and a discretization of the source terms. Moreover, it is possible to encode this averaging process into a larger relaxation system so that the flux splitting method and the source term discretization can also be considered as a direct approximation of the relaxation system. That new angle of analysis will enable to prove the preservation of admissible states and a discrete entropy inequality, under Courant-Friedrichs-Lewy (CFL) constraints along with the well-balanced properties. Moreover, following similar lines as in [27, 29] we will also derive a modified scheme that preserves accuracy in the low Mach regime.

The paper is organized as follows: we first introduce the set of equations with the thermodynamical related hypotheses that support the stability properties of the model and we present the stationary profiles we will be interested in. Then, anticipating all the technical developments that are used to derive the numerical scheme, we will directly present the overall resulting discretization. Next, we will present the equivalence between the flux-splitting approach and both an averaging process and a relaxation approximation. This will allow us to separately build on one hand a discretization for the source terms and pressure related fluxes and on the other hand advection fluxes. Then we will propose a simple analysis of the low Mach behavior of the scheme using a truncation error analysis that will suggest a modification of the pressure related flux. We will then examine the properties of the numerical scheme including a proof of a discrete entropy inequality. We also propose two alternatives approximation of the gravitational energy source term that the reader may want to use depending on the field of application. Finally, we present one-dimensional and two-dimensional numerical experiments that demonstrate the good behavior of the scheme.

2 Flow model

For the sake of clarity but without loss of generality, we focus on one-dimensional problems and we consider the Euler equations supplemented with a potential source term, that is to say

$$\partial_t \mathbf{U} + \partial_x \mathbf{F}(\mathbf{U}) = \mathbf{S}(\mathbf{U}, \phi), \quad \text{for } x \in \mathbb{R}, t > 0, \quad (1)$$

with $\mathbf{U} = (\rho, \rho u, \rho E)^T$, $\mathbf{F}(\mathbf{U}) = (\rho u, \rho u^2 + p, \rho u E + p u)^T$ and $\mathbf{S}(\mathbf{U}, \phi) = -\rho \partial_x \phi(0, 1, u)^T$. Although (1) is not strictly limited to flows accounting for gravitational forces the stationary potential $x \mapsto \phi(x)$ will be referred to as the gravitational potential. The fields ρ , u , p and E respectively denote the density, velocity, pressure and specific total energy of the fluid. If $e = E - u^2/2$ is the specific internal energy, we define the set of admissible states

$$\Omega = \{(\rho, \rho u, \rho E) \in \mathbb{R}^3 \mid \rho > 0, e > 0\}. \quad (2)$$

Let s be the specific entropy of the fluid, we suppose given an Equation Of State (EOS) in the form of a mapping $(1/\rho, s) \mapsto e^{\text{EOS}}(1/\rho, s)$ that satisfies the classic Weyl assumptions [30, 27]:

$$\frac{\partial e^{\text{EOS}}}{\partial(1/\rho)} < 0, \quad \frac{\partial e^{\text{EOS}}}{\partial s} > 0, \quad \frac{\partial^2 e^{\text{EOS}}}{\partial(1/\rho)^2} > 0, \quad (3a)$$

$$\frac{\partial^2 e^{\text{EOS}}}{\partial s^2} > 0, \quad \left[\frac{\partial^2 e^{\text{EOS}}}{\partial(1/\rho)^2} \right] \left[\frac{\partial^2 e^{\text{EOS}}}{\partial s^2} \right] > \left[\frac{\partial^2 e^{\text{EOS}}}{\partial s \partial(1/\rho)} \right]^2, \quad \frac{\partial^3 e^{\text{EOS}}}{\partial(1/\rho)^3} < 0. \quad (3b)$$

The temperature T and the pressure p of the fluids are related to the other parameters respectively by $T = T^{\text{EOS}}(1/\rho, s) = \partial e^{\text{EOS}} / \partial s$ and $p = p^{\text{EOS}}(1/\rho, s) = -\partial e^{\text{EOS}} / \partial(1/\rho)$. It is possible to define a mapping $(1/\rho, e) \mapsto s^{\text{EOS}}(1/\rho, e)$ such that $e = e^{\text{EOS}}(1/\rho, s)$ if $s = s^{\text{EOS}}(1/\rho, e)$ so that we have the Gibbs relation

$$de + p d(1/\rho) = T ds. \quad (4)$$

Note that (3) imply that $-s^{\text{EOS}}(1/\rho, e)$ and $e^{\text{EOS}}(1/\rho, s)$ are strictly convex functions. Relations (3) also ensure that

$$\frac{\partial p^{\text{EOS}}}{\partial(1/\rho)}(1/\rho, s) < 0, \quad (5)$$

so that the sound velocity $c = 1/\rho\sqrt{\partial p^{\text{EOS}}(1/\rho, s)/\partial(1/\rho)}$ is real valued. We also make the classic assumption [31] that

$$\mathcal{M}s(\mathcal{V}|\mathcal{M}, \mathcal{E}|\mathcal{M}) = S(\mathcal{M}, \mathcal{V}, \mathcal{E}), \quad (6)$$

where the entropy $(\mathcal{M}, \mathcal{V}, \mathcal{E}) \mapsto S(\mathcal{M}, \mathcal{V}, \mathcal{E})$ is a strictly concave homogeneous first order function. Let us note that as $\frac{\partial S}{\partial \mathcal{E}}(\mathcal{M}, \mathcal{V}, \mathcal{E}) = \frac{\partial s}{\partial e}(\mathcal{V}|\mathcal{M}, \mathcal{E}|\mathcal{M}) = 1/T^{\text{EOS}}(\mathcal{V}|\mathcal{M}, \mathcal{E}|\mathcal{M}) > 0$, then $\mathcal{E} \mapsto S(\mathcal{M}, \mathcal{V}, \mathcal{E})$ is a strictly increasing function.

Weak solutions of (1) also satisfy the entropy inequality

$$\partial_t(\rho s) + \partial_x(u\rho s) \geq 0, \quad (7)$$

where the inequality (7) is indeed an equality in the case of smooth solutions (see [32, 33, 34, 35]).

In this work, we will also be interested in the study of particular steady states solutions of (1) called the hydrostatic equilibria that are defined by

$$\partial_x p = -\rho \partial_x \phi, \quad u = 0. \quad (8)$$

Moreover, we will investigate finite volume methods for approximating (1) that are compatible with discrete equivalents of (7) and (8) while ensuring that the fluid states remain in Ω .

Before going any further, we introduce the following decomposition of the flux \mathbf{F}

$$\mathbf{F}(\mathbf{U}) = \mathbf{P}(\mathbf{U}, p^{\text{EOS}}(1/\rho, e)) + \mathbf{A}(\mathbf{U}, u), \quad \mathbf{P}(\mathbf{U}, p') = (0, p', p'u)^T, \quad \mathbf{A}(\mathbf{U}, v) = v\mathbf{U}, \quad (9)$$

into two parts \mathbf{P} and \mathbf{A} that account respectively for the pressure and the advection effects.

3 Approximation of the flow model by a flux-splitting strategy

Let us introduce the notations for our space-time discretization: we consider a strictly increasing sequence $(x_{j+1/2})_{j \in \mathbb{Z}}$ and divide the real line into cells where the j^{th} cell is the interval $[x_{j-1/2}, x_{j+1/2}]$. The space step of j^{th} cell is $\Delta x_j = x_{j+1/2} - x_{j-1/2} > 0$. We note $\Delta t > 0$ the time step such that $t^{n+1} - t^n = \Delta t$ with $n \in \mathbb{N}$. For a given initial condition $x \mapsto \mathbf{U}^0(x)$, we consider a discrete initial data \mathbf{U}_j^0 defined by $\mathbf{U}_j^0 = \frac{1}{\Delta x_j} \int_{x_{j-1/2}}^{x_{j+1/2}} \mathbf{U}^0(x) dx$, for $j \in \mathbb{Z}$. The algorithm proposed in this paper aims at computing a first order accurate (in both space and time) approximation of the cell-averaged values \mathbf{U}_j^n of $\frac{1}{\Delta x_j} \int_{x_{j-1/2}}^{x_{j+1/2}} \mathbf{U}(x, t^n) dx$ where $x \mapsto \mathbf{U}(x, t^n)$ is the exact solution of (1) at time t^n .

The aim of our work is to propose a conservative finite volume discretization in (1) in the form

$$\mathbf{U}_j^{n+1} - \mathbf{U}_j^n + \frac{\Delta t}{\Delta x_j} (\mathbf{F}_{j+1/2} - \mathbf{F}_{j-1/2}) = \Delta t \mathbf{S}_j, \quad (10a)$$

where the numerical flux $\mathbf{F}_{j+1/2}$ can be expressed thanks to a flux splitting strategy along the lines of [8, 7, 14] as the sum

$$\mathbf{F}_{j+1/2} = \mathbf{P}_{j+1/2} + \mathbf{A}_{j+1/2} \quad (10b)$$

of an acoustic flux $\mathbf{P}_{j+1/2}$ and an advection flux $\mathbf{A}_{j+1/2}$ that are respectively an approximate value for \mathbf{P} and \mathbf{A} at $x = x_{j+1/2}$.

Before going any further, let us display the final flux and source term formulas that will result from the developments in the forthcoming sections: if we note $\Pi_j^n = p^{\text{EOS}}(1/\rho_j^n, e_j^n)$ then $\mathbf{P}_{j+1/2}$, $\mathbf{A}_{j+1/2}$ and \mathbf{S}_j are evaluated as

$$\mathbf{P}_{j+1/2} = [0, \Pi_{j+1/2}^*, \Pi_{j+1/2}^* u_{j+1/2}^*]^T, \quad \mathbf{A}_{j+1/2} = (u_{j+1/2}^*)^+ \mathbf{U}_j^n + (u_{j+1/2}^*)^- \mathbf{U}_{j+1}^n, \quad (11a)$$

$$\mathbf{S}_j = \frac{\Delta x_{j+1/2}}{2\Delta x_j} \mathbf{S}_{j+1/2} + \frac{\Delta x_{j-1/2}}{2\Delta x_j} \mathbf{S}_{j-1/2}, \quad \Delta x_{j+1/2} = \frac{1}{2}(\Delta x_j + \Delta x_{j+1}), \quad (11b)$$

with

$$u_{j+1/2}^* = \frac{1}{2}(u_j^n + u_{j+1}^n) - \frac{1}{2a_{j+1/2}}(\Pi_{j+1}^n - \Pi_j^n) - \frac{1}{2a_{j+1/2}}\left(\frac{\rho_j^n + \rho_{j+1}^n}{2}\right)(\phi_{j+1} - \phi_j), \quad (12a)$$

$$\Pi_{j+1/2}^* = \frac{1}{2}(\Pi_j^n + \Pi_{j+1}^n) - \frac{a_{j+1/2}}{2}(u_{j+1}^n - u_j^n), \quad (12b)$$

$$\mathbf{S}_{j+1/2} = -\frac{\rho_j^n + \rho_{j+1}^n}{2} \left(\frac{\phi_{j+1} - \phi_j}{\Delta x_{j+1/2}} \right) [0, 1, u_{j+1/2}^n]^T. \quad (12c)$$

The term $a_{j+1/2}$ that features in (12) is an approximate acoustic impedance at $x_{j+1/2}$ whose definition will be specified later. It is worth mentioning that the scheme defined by (12) shares strong similarities with the Zha-Bilgen scheme [7] in the homogeneous case $\mathbf{S} = \mathbf{0}$. Other connection can also be drawn: the flux $\mathbf{P}_{j+1/2}$ is the flux obtained for the acoustic system used in operator splitting method presented in [27] of the acoustic scheme for the gas dynamics in Lagrangian coordinates [36]. The flux $\mathbf{A}_{j+1/2}$ involves a simple upwind choice with respect to the material velocity. Although (12) seem a sensible discretization of (9) that is easy to implement, we will motivate these choices in the next sections using technical developments that will shed light on interesting properties of the scheme.

3.1 Flux splitting as an averaging process and a relaxation approximation

The first step of our analysis of (12) is to highlight a connection between the flux splitting approach and a relaxation approximation. Indeed, one can remark that (10) can be reformulated into

$$\mathbf{U}_j^{n+1} = \frac{\mathbf{U}_j^P + \mathbf{U}_j^A}{2}, \quad (13a)$$

where \mathbf{U}_j^P and \mathbf{U}_j^A are defined by

$$\mathbf{U}_j^P - \mathbf{U}_j^n + \frac{\Delta t}{\Delta x_j} [2\mathbf{P}_{j+1/2} - 2\mathbf{P}_{j-1/2}] = 2\Delta t \mathbf{S}_j, \quad (13b)$$

$$\mathbf{U}_j^A - \mathbf{U}_j^n + \frac{\Delta t}{\Delta x_j} [2\mathbf{A}_{j+1/2} - 2\mathbf{A}_{j-1/2}] = \mathbf{0}. \quad (13c)$$

Relation (13a) indicates that the flux splitting (10b) can be viewed as an averaging process. Moreover, the update relations (13b)-(13c) suggest that \mathbf{U}_j^P and \mathbf{U}_j^A can be defined as approximate solutions of two systems that respectively only account for the pressure and the advection effects.

We propose to formalize the averaging process of (13) thanks to a relaxation approximation. Let ν be a positive parameter and consider the system

$$\partial_t \begin{bmatrix} \mathbf{U}^P \\ \rho^P \Pi^P \\ \rho^P \mathcal{T}^P \\ \phi \end{bmatrix} + \partial_x \begin{bmatrix} 2\mathbf{P}(\mathbf{U}^P, \Pi^P) \\ 2a^2 u^P \\ -2u^P \\ 0 \end{bmatrix} - \begin{bmatrix} 2\mathbf{S}(\mathbf{U}^P, \phi) \\ 0 \\ 0 \\ 0 \end{bmatrix} = \frac{\nu}{2} \begin{bmatrix} 2\mathbf{U}^P - (\mathbf{U}^P + \mathbf{U}^A) \\ p^{\text{EOS}}(1/\rho^P, e^P) - \Pi^P \\ 1 - \rho^P \mathcal{T}^P \\ 0 \end{bmatrix}, \quad (14a_\nu)$$

$$\partial_t \begin{bmatrix} \mathbf{U}^A \\ \rho^A \Pi^A \\ \rho^A \mathcal{T}^A \end{bmatrix} + \partial_x \begin{bmatrix} 2\mathbf{A}(\mathbf{U}^A, u^P) \\ 2\rho^A \Pi^A u^P \\ 2u^P \end{bmatrix} = \frac{\nu}{2} \begin{bmatrix} 2\mathbf{U}^A - (\mathbf{U}^P + \mathbf{U}^A) \\ p^{\text{EOS}}(1/\rho^A, e^A) - \Pi^A \\ 1 - \rho^A \mathcal{T}^A \end{bmatrix}. \quad (14b_\nu)$$

The system (14_ν) features a pair of duplicate conservative variable ($\mathbf{U}^P, \mathbf{U}^A$) and 4 other variables: $\Pi^P, \Pi^A, \mathcal{T}^A$ and \mathcal{T}^P . The variables Π^P and Π^A are surrogate for the thermodynamical pressure, while \mathcal{T}^A and \mathcal{T}^P play the role of a pseudo-specific volume. It is possible to view (14_ν) as a Suliciu relaxation approximation with a separation of the acoustic and transport operators. Indeed, (14_ν) implies that

$$\partial_t \left[\frac{\mathbf{U}^P + \mathbf{U}^A}{2} \right] + \partial_x [\mathbf{P}(\mathbf{U}^P, \Pi^P) + \mathbf{A}(\mathbf{U}^A, u^P)] = \mathbf{S}(\mathbf{U}^P, \phi), \quad (15a)$$

$$\partial_t \left[\frac{\rho^P \Pi^P + \rho^A \Pi^A}{2} \right] + \partial_x (\rho^A \Pi^A u^P + a^2 u^P) = \nu \left(\frac{p^{\text{EOS}}(1/\rho^A, e^A) + p^{\text{EOS}}(1/\rho^P, e^P)}{2} - \frac{\Pi^A + \Pi^P}{2} \right), \quad (15b)$$

$$\partial_t \left[\frac{\rho^P \mathcal{T}^P + \rho^A \mathcal{T}^A}{2} \right] = \nu \left(1 - \frac{\rho^P \mathcal{T}^P + \rho^A \mathcal{T}^A}{2} \right). \quad (15c)$$

Taking the limit $\nu \rightarrow +\infty$ formally enforces that $\mathbf{U}^P = \mathbf{U}^A = \mathbf{U} = (\rho, \rho u, \rho E)^T$ and $\Pi^A = \Pi^P = p^{\text{EOS}}(1/\rho, e)$, so that (15a) yields

$$\partial_t \mathbf{U} + \partial_x [\mathbf{P}(\mathbf{U}, p^{\text{EOS}}(1/\rho, e)) + \mathbf{A}(\mathbf{U}, u)] = \mathbf{S}(\mathbf{U}, \phi), \quad (16)$$

By (9) we see that we recover the Euler system (1). Therefore, we choose to use the relaxation system (14_ν) as an approximation of (1) in the limit $\nu \rightarrow +\infty$. The parameter $a > 0$ is a constant approximate value of the acoustic impedance ρc that has to be chosen sufficiently large for stability concerns that we will be discussed later (see (38)). The equation (15b) plays here a similar role as surrogate pressure equation in the classic Suliciu approximation [37, 38, 39]. The sole purpose of equation (15c) is to ensure that $\frac{\rho^P \mathcal{T}^P + \rho^A \mathcal{T}^A}{2} = 1$ in the regime

$\nu \rightarrow \infty$. In our discretization strategy, we classically mimic the $\nu \rightarrow \infty$ regime for $t \in [t^n, t^{n+1})$, by enforcing $(\mathbf{U}^P, \Pi^P, \mathcal{T}^A, \mathbf{U}^A, \Pi^A, \mathcal{T}^A)(t = t^n) = (\mathbf{U}, p^{\text{EOS}}(1/\rho, e), 1/\rho, \mathbf{U}, p^{\text{EOS}}(1/\rho, e), 1/\rho)(t = t^n)$ and by solving the relaxation off-equilibrium system $(14_{\nu=0})$.

We now turn to the properties of the off-equilibrium system $(14_{\nu=0})$ with the following proposition whose proof is given in B.

Proposition 3.1. *The system $(14_{\nu=0})$ is hyperbolic with a set of characteristic velocities given by: $2u^P$ (with an algebraic multiplicity 4), 0 (with an algebraic multiplicity 5) and $\pm 2a/\rho^P$. Moreover, $(14_{\nu=0})$ only involves linearly degenerate fields.*

The relaxation formulation (14_{ν}) shows that the flux we propose here shares similarities with the operator acoustic/-transport splitting strategy presented in [27, 19]. Indeed, the source term and pressure effects are treated together apart from the advection terms. The difference is that although the operators are separated that are distributed within a larger system instead of two isolated systems. We will see in the next sections approximations of each of these subsystems that will enable to retrieve (12).

3.2 Derivation of the numerical fluxes

We will now use a discretization of system $(14_{\nu=0})$ in order to build the fluxes $\mathbf{P}_{j+1/2}$ and $\mathbf{A}_{j+1/2}$ of our splitting strategy (10). Before going any further, let us underline once again that we will consider the evolution of \mathcal{T}^A and \mathcal{T}^P and the update of discrete associated values although these variables do not play any role in the update relation of our flux splitting scheme (11). Nevertheless, these variables will help us in constructing discrete entropy inequalities verified by the numerical scheme.

We consider the first 4 equations of $(14_{\nu=0})$ that form a first independant subsystem for the acoustic part

$$\partial_t \begin{bmatrix} \mathbf{U}^P \\ \rho^P \Pi^P \\ \rho^P \mathcal{T}^P \\ \phi \end{bmatrix} + \partial_x \begin{bmatrix} 2\mathbf{P}(\mathbf{U}^P, \Pi^P) \\ 2a^2 u^P \\ -2u^P \\ 0 \end{bmatrix} - \begin{bmatrix} 2\mathcal{S}(\mathbf{U}^P, \phi) \\ 0 \\ 0 \\ 0 \end{bmatrix} = \begin{bmatrix} \mathbf{0} \\ 0 \\ 0 \\ 0 \end{bmatrix}. \quad (17a)$$

Then we remark that the update of the conservative variable $(\mathbf{U}^A + \mathbf{U}^P)/2$ by (15a) does not involve Π^A that acts as a passive variable, we will examine a second subsystem for the advection effects that reads

$$\partial_t \begin{bmatrix} \mathbf{U}^A \\ \rho^A \mathcal{T}^A \end{bmatrix} + \partial_x \begin{bmatrix} 2\mathbf{A}(\mathbf{U}^A, u^P) \\ 2u^P \end{bmatrix} = \mathbf{0}. \quad (18a)$$

The initial conditions for (17a) (18a) will verify $(\mathbf{U}^P, \Pi^P, \phi, \mathcal{T}^P)(t = 0, x) = (\mathbf{U}_j^n, p^{\text{EOS}}(1/\rho_j^n, e_j^n), \phi_i, 1/\rho_j^n)$ and $(\mathbf{U}^A, \mathcal{T}^A)(t = 0, x) = (\mathbf{U}_j^n, 1/\rho_j^n)$ for $x \in (x_{j-1/2}, x_{j+1/2})$.

Using similar lines as in [19], we propose to build the numerical update (13b) by using an approximate Riemann solver $(\mathbf{U}_{\text{RP}}, \Pi_{\text{RP}}, \mathcal{T}_{\text{RP}})$ for (17a). The detailed building process of $(\mathbf{U}_{\text{RP}}, \Pi_{\text{RP}}, \mathcal{T}_{\text{RP}})$ is given in the appendix C. Updating $(\mathbf{U}^P, \rho^P \mathcal{T}^P)$ thanks to this approximate Riemann solver is equivalent to the following update formula:

$$\begin{bmatrix} \mathbf{U}_j^P \\ \rho_j^P \mathcal{T}_j^P \end{bmatrix} = \begin{bmatrix} \mathbf{U}_j^n \\ 1 \end{bmatrix} - \frac{\Delta t}{\Delta x_j} \begin{bmatrix} 2\mathbf{P}_{j+1/2}^* - 2\mathbf{P}_{j-1/2}^* \\ -2u_{j+1/2}^* + 2u_{j-1/2}^* \end{bmatrix} + \begin{bmatrix} 2\Delta t \mathbf{S}_j \\ 0 \end{bmatrix}, \quad (19)$$

where the discrete fluxes and source terms are defined by

$$\mathbf{P}_{j+1/2}^* = [0, \Pi_{j+1/2}^*, \Pi_{j+1/2}^* u_{j+1/2}^*]^T, \quad \mathbf{S}_j = \frac{\Delta x_{j+1/2}}{2\Delta x_j} \mathbf{S}_{j+1/2} + \frac{\Delta x_{j-1/2}}{2\Delta x_j} \mathbf{S}_{j-1/2}, \quad (20a)$$

with

$$u_{j+1/2}^* = \frac{1}{2}(u_j^n + u_{j+1}^n) - \frac{1}{2a_{j+1/2}}(\Pi_{j+1}^n - \Pi_j^n) - \frac{1}{2a_{j+1/2}}\left(\frac{\rho_j^n + \rho_{j+1}^n}{2}\right)(\phi_{j+1} - \phi_j), \quad (20b)$$

$$\Pi_{j+1/2}^* = \frac{1}{2}(\Pi_j^n + \Pi_{j+1}^n) - \frac{a_{j+1/2}}{2}(u_{j+1}^n - u_j^n), \quad (20c)$$

$$\mathbf{S}_{j+1/2} = -\frac{\rho_j^n + \rho_{j+1}^n}{2} \left(\frac{\phi_{j+1} - \phi_j}{\Delta x_{j+1/2}} \right) [0, 1, u_{j+1/2}^*]^T, \quad (20d)$$

so that we indeed retrieve the discrete flux and discrete source term evaluation of (12).

Under the Courant-Friedrichs-Lewy (CFL) condition

$$\frac{\Delta t}{\Delta x_j} \max_{j \in \mathbb{Z}} \left(\max \left(1/\rho_j^n, 1/\rho_{j+1}^n \right) a_{j+1/2} \right) \leq \frac{1}{4}, \quad (21)$$

the update relations (19) are stable in the sense that the waves involved in the approximate Riemann solver centered each cell interface $x_{j+1/2}$ will not interact with each other. The parameter $a_{j+1/2}$ is a local choice of the artificial acoustic impedance a associated with each interface $j + 1/2$ that should be chosen large enough so that (21) can guarantee stability for (19). In practice, we define it by setting

$$a_{j+1/2} = K \max \left(\rho_j^n c_j^n, \rho_{j+1}^n c_{j+1}^n \right) \quad \text{with } K > 1. \quad (22)$$

We now turn to the definition of the fluxes for the advection subsystem (18a): we simply use a standard finite-volume upwind update formula by setting:

$$\begin{bmatrix} U_j^A \\ \rho^A \mathcal{T}^A \end{bmatrix} = \begin{bmatrix} U_j^n \\ 1 \end{bmatrix} - \frac{\Delta t}{\Delta x_j} \begin{bmatrix} 2\mathbf{A}_{j+1/2} - 2\mathbf{A}_{j-1/2} \\ 2u_{j+1/2}^* - 2u_{j-1/2}^* \end{bmatrix}, \quad (23a)$$

with

$$\mathbf{A}_{j+1/2} = (u_{j+1/2}^*)^+ U_j^n + (u_{j+1/2}^*)^- U_{j+1}^n, \quad (23b)$$

where $u_{i \pm 1/2}^*$ is given by (20b) and $b^\pm = (b \pm |b|)/2$ for any scalar b . For (23), we consider the classic CFL constraint

$$\frac{\Delta t}{\Delta x_j} 2 \max_{j \in \mathbb{Z}} \left[\left(u_{j+1/2}^* \right)^+ - \left(u_{j-1/2}^* \right)^- \right] < 1. \quad (24)$$

We also consider a discrete update of the variable $(\rho \mathcal{T})^A$ by setting

$$(\rho \mathcal{T})_j^A = 1 - 2 \frac{\Delta t}{\Delta x_j} [(u_{j+1/2}^*) - (u_{j-1/2}^*)]. \quad (25)$$

It is possible to consider the flux splitting scheme as a two-step evaluation followed by an average: given the states U_j^n , $j \in \mathbb{Z}$:

1. Compute U_j^P thanks to (19),
2. Compute U_j^A thanks to (23),
3. Update the discrete state value by evaluating $U_j^{n+1} = (U_j^P + U_j^A)/2$.

Then, we see that the overall update reads

$$U_j^{n+1} - U_j^n + \frac{\Delta t}{\Delta x_j} [(\mathbf{A}_{j+1/2} + \mathbf{P}_{j+1/2}) - (\mathbf{A}_{j-1/2} + \mathbf{P}_{j-1/2})] = \Delta t \mathbf{S}_j, \quad (26)$$

so that we retrieve the discretization (10).

The properties of the numerical schemes (19), (23) and (26) are given in section 5.

4 Behavior in the low Mach regime and modified numerical scheme

In this section, we investigate the behavior of the flux splitting scheme (26) in the low Mach regime along the lines used in [27]. In order to outline the dependence on the system on the Mach number, we first recall a classic rescaling of (1) thanks to the following non-dimensional numbers

$$\tilde{x} = \frac{x}{L}, \quad \tilde{t} = \frac{t}{t_0}, \quad \tilde{\rho} = \frac{\rho}{\rho_0}, \quad \tilde{u} = \frac{u}{u_0}, \quad \tilde{e} = \frac{e}{e_0}, \quad \tilde{p} = \frac{p}{p_0}, \quad \widetilde{(\partial_x \phi)} = \frac{\partial_x \phi}{(\partial_x \phi)_0}. \quad (27)$$

The numbers L , t_0 , ρ_0 , u_0 , p_0 , $e_0 = p_0/\rho_0$, $c_0 = \sqrt{p_0/\rho_0}$ and $(\partial_x \phi)_0$ featuring in (27) are respectively characteristic magnitudes for length, time, density, velocity, pressure, sound velocity and $\partial_x \phi$ the gravitationnal force,. The Mach

number M and the Froude number Fr are defined by $M = u_0/c_0$ and $Fr = u_0/\sqrt{L(\partial_x \phi)_0}$, so that the system (1) takes the following non-dimensional form

$$\partial_{\tilde{t}} \tilde{\rho} + \partial_{\tilde{x}}(\tilde{\rho} \tilde{u}) = 0, \quad (28a)$$

$$\partial_{\tilde{t}}(\tilde{\rho} \tilde{u}) + \partial_{\tilde{x}}(\tilde{\rho} \tilde{u}^2) + \frac{1}{M^2} \partial_{\tilde{x}} \tilde{p} = -\frac{1}{Fr^2} \widetilde{\rho(\partial_x \phi)}, \quad (28b)$$

$$\partial_{\tilde{t}}(\tilde{\rho} \tilde{E}) + \partial_{\tilde{x}}(\tilde{\rho} \tilde{E} \tilde{u} + \tilde{p} \tilde{u}) = -\frac{M^2}{Fr^2} \widetilde{\tilde{\rho} \tilde{u}(\partial_x \phi)}. \quad (28c)$$

For a fixed value of Fr , in the low Mach regime, the term $\partial_{\tilde{x}} \tilde{p}$ should remain of magnitude $O(M^2)$ in order to (28) to remain non-singular. Following [27] we will express the numerical scheme using non dimensional quantities and examine the dependency of the truncation error on the Mach number. To achieve this task, we suppose that the discretized variables verify a discrete equivalent of the low Mach regime hypothesis: $\tilde{\Pi}_{j+1}^n = \tilde{\Pi}_j^n + O(M^2 \Delta \tilde{x})$ and express the schemes (19), (23) and (26) using non-dimensional variables. The resulting truncation errors are given in the following proposition.

Proposition 4.1. *For a fixed value of Fr and a discretized set of variables in the (discrete) low Mach regime, the non-dimensional discretization of the pressure subsystem (19) is consistent with*

$$\partial_{\tilde{t}} \tilde{\rho}^P = 0, \quad (29a)$$

$$\partial_{\tilde{t}}(\tilde{\rho}^P \tilde{u}^P) + \frac{2}{M^2} \partial_{\tilde{x}} \tilde{p}^P = -\frac{2}{Fr^2} \tilde{\rho}^P \widetilde{(\partial_x \phi)} + O(\Delta \tilde{t}) + O\left(\frac{\Delta \tilde{x}}{M}\right), \quad (29b)$$

$$\partial_{\tilde{t}}(\tilde{\rho}^P \tilde{E}^P) + 2(\tilde{p}^P \tilde{u}^P) = -2\frac{M^2}{Fr^2} \tilde{\rho}^P \tilde{u}^P \widetilde{(\partial_x \phi)} + O(\Delta \tilde{t}) + O(M \Delta \tilde{x}), \quad (29c)$$

and the non-dimensional discretization of the advection subsystem (23) is consistent with

$$\partial_{\tilde{t}} \tilde{b}^A + 2\partial_{\tilde{x}}(\tilde{b}^A \tilde{u}^P) = O(\Delta \tilde{t}) + O(\Delta \tilde{x}) + O(M \Delta \tilde{x}), \quad \tilde{b}^A \in \{\tilde{\rho}^A, \widetilde{(\rho u)^A}, \widetilde{(\rho E)^A}\} \quad (29d)$$

The overall discretization (26) is equivalent to

$$\partial_{\tilde{t}} \tilde{\rho} + \partial_{\tilde{x}}(\tilde{\rho} \tilde{u}) = O(\Delta \tilde{t}) + O(\Delta \tilde{x}) + O(M \Delta \tilde{x}), \quad (30a)$$

$$\partial_{\tilde{t}}(\tilde{\rho} \tilde{u}) + \partial_{\tilde{x}}(\tilde{\rho} \tilde{u}^2) + \frac{1}{M^2} \partial_{\tilde{x}} \tilde{p} = -\frac{1}{Fr^2} \tilde{\rho} \widetilde{(\partial_x \phi)} + O(\Delta \tilde{t}) + O(\Delta \tilde{x}) + O(M \Delta \tilde{x}) + O\left(\frac{\Delta \tilde{x}}{M}\right), \quad (30b)$$

$$\partial_{\tilde{t}}(\tilde{\rho} \tilde{E}) + \partial_{\tilde{x}}(\tilde{\rho} \tilde{E} \tilde{u} + \tilde{p} \tilde{u}) = -\frac{M^2}{Fr^2} \tilde{\rho} \tilde{u} \widetilde{(\partial_x \phi)} + O(\Delta \tilde{t}) + O(\Delta \tilde{x}) + O(M \Delta \tilde{x}). \quad (30c)$$

Similarly as in [27], the error term of magnitude $O(\Delta \tilde{x}/M)$ that appears in (29b) and (30b) results from the non-centered term evaluated in the discretized pressure (20c). In order to prevent this term from being very large when $M \ll \Delta \tilde{x}$. We use a similar cure as in [27] that consists in replacing $\Pi_{j+1/2}$ by

$$\Pi_{j+1/2}^{*,\theta} = \frac{1}{2} (\Pi_j^n + \Pi_{j+1}^n) - \theta_{j+1/2} \frac{a_{j+1/2}}{2} (u_{j+1}^n - u_j^n), \quad (31)$$

so that the acoustic subsystem (17a) is now approximated by

$$\mathbf{U}^P = \mathbf{U}_j^n - \frac{\Delta t}{\Delta x_j} [2\mathbf{P}_{j+1/2}^\theta - 2\mathbf{P}_{j-1/2}^\theta] + 2\Delta t \mathbf{S}_j, \quad (32a)$$

$$\mathbf{P}_{j+1/2}^\theta = \left[0, \Pi_{j+1/2}^\theta, \Pi_{j+1/2}^\theta u_{j+1/2} \right]^T, \quad (32b)$$

and the overall scheme reads

$$\mathbf{U}_j^{n+1} - \mathbf{U}_j^n + \frac{\Delta t}{\Delta x_j} \left[(\mathbf{A}_{j+1/2} + \mathbf{P}_{j+1/2}^\theta) - (\mathbf{A}_{j-1/2} + \mathbf{P}_{j-1/2}^\theta) \right] = \Delta t \mathbf{S}_j. \quad (33)$$

The behavior of (33) in the low Mach regime is summed up in the following proposition.

Proposition 4.2. *For a fixed value of Fr and a discretized set of variables in the (discrete) low Mach regime, the non-dimensional discretization of the pressure subsystem (19) is consistent with*

$$\partial_{\tilde{t}} \tilde{\rho}^P = 0, \quad (34a)$$

$$\partial_{\tilde{t}}(\tilde{\rho}^P \tilde{u}^P) + \frac{2}{M^2} \partial_{\tilde{x}} \tilde{p}^P = -\frac{2}{Fr^2} \tilde{\rho}^P \widetilde{(\partial_x \phi)} + O(\Delta \tilde{t}) + O\left(\frac{\theta \Delta \tilde{x}}{M}\right), \quad (34b)$$

$$\partial_{\tilde{t}}(\tilde{\rho}^P \tilde{E}^P) + 2(\tilde{p}^P \tilde{u}^P) = -2\frac{M^2}{Fr^2} \tilde{\rho}^P \tilde{u}^P \widetilde{(\partial_x \phi)} + O(\Delta \tilde{t}) + O(M \Delta \tilde{x}) + O(\theta M \Delta \tilde{x}). \quad (34c)$$

For the transport subsystem discretization, the truncation error estimate associated with the modified scheme is the same as in (29d), we have

$$\partial_{\tilde{t}} \tilde{b}^A + 2\partial_{\tilde{x}}(\tilde{b}^A \tilde{u}^P) = O(\Delta \tilde{t}) + O(\Delta \tilde{x}) + O(M \Delta \tilde{x}), \quad \tilde{b}^A \in \{\tilde{\rho}^A, \widetilde{(\rho u)}^A, \widetilde{(\rho E)}^A\}. \quad (35)$$

The overall discretization (26) is equivalent to

$$\partial_{\tilde{t}} \tilde{\rho} + \partial_{\tilde{x}}(\tilde{\rho} \tilde{u}) = O(\Delta \tilde{t}) + O(\Delta \tilde{x}) + O(M \Delta \tilde{x}), \quad (36a)$$

$$\partial_{\tilde{t}}(\tilde{\rho} \tilde{u}) + \partial_{\tilde{x}}(\tilde{\rho} \tilde{u}^2) + \frac{1}{M^2} \partial_{\tilde{x}} \tilde{p} = -\frac{1}{\text{Fr}^2} \tilde{\rho}(\partial_{\tilde{x}} \phi) + O(\Delta \tilde{t}) + O(\Delta \tilde{x}) + O(M \Delta \tilde{x}) + O\left(\theta \frac{\Delta \tilde{x}}{M}\right), \quad (36b)$$

$$\partial_{\tilde{t}}(\tilde{\rho} \tilde{E}) + \partial_{\tilde{x}}(\tilde{\rho} \tilde{E} \tilde{u} + \tilde{p} \tilde{u}) = -\frac{M^2}{\text{Fr}^2} \tilde{\rho} \tilde{u}(\partial_{\tilde{x}} \phi) + O(\Delta \tilde{t}) + O(\Delta \tilde{x}) + O(M \Delta \tilde{x}) + O(\theta M \Delta \tilde{x}). \quad (36c)$$

Thanks to (36) we can see that if the magnitude of the parameter θ is $O(M)$ then the truncation error of (36) is uniform with respect to M .

5 Properties of the flux splitting schemes

In this section, we will derive properties for both the modified pressure update (32a) and the advection scheme (23) that will enable properties for the full flux splitting scheme (33). Before going any further, we consider a discretization of the hydrostatic pressure stationary state (8) defined by

$$\Pi_{j+1} - \Pi_j = -\frac{\rho_{j+1} + \rho_j}{2}(\phi_{j+1} - \phi_j), \quad u_j = 0, \quad \forall j \in \mathbb{Z}. \quad (37)$$

For the pressure subsystem, the properties of the discretization result from the properties of the approximate Riemann solver that are detailed in C. Using the notations of the definition (86), we consider the following more restricting subcharacteristic conditions

$$\mathcal{T}_L^* > 0, \quad -\partial_{\mathcal{T}} p^{\text{EOS}}(\mathcal{T}, s_L) \leq a^2, \quad \forall \mathcal{T} \in I(\mathcal{T}_L, \mathcal{T}_L^*), \quad (38a)$$

$$\mathcal{T}_R^* > 0, \quad -\partial_{\mathcal{T}} p^{\text{EOS}}(\mathcal{T}, s_R) \leq a^2, \quad \forall \mathcal{T} \in I(\mathcal{T}_R, \mathcal{T}_R^*), \quad (38b)$$

We have the following proposition.

Proposition 5.1. *The all-Mach discretization (32a) of the pressure subsystem verifies the following properties.*

1. *The pressure subsystem all-mach discretization (32a) is well-balanced in the sense that it preserves discrete hydrostatic solutions defined by (37), for any $\theta \in [0, 1]$.*
2. *Suppose that a is chosen large enough so that (38) is verified: under the CFL condition (21), if $\rho_j^n > 0$ for all $j \in \mathbb{Z}$, then $\mathcal{T}_j^P > 0$ for all $j \in \mathbb{Z}$, for any $\theta \in [0, 1]$.*
3. *If $\theta = O(M)$ (e.g. via (40)), then the truncation error of the scheme (32a) is uniform with respect to M when $M \ll 1$.*
4. *Suppose that a is chosen large enough so that (38) is verified and that (110) is valid: under the CFL conditions (21) we have that*

(a) *for all $j \in \mathbb{Z}$ we have $e_j^P > 0$,*

(b) *the discretization (32a) satisfies the following inequality that involves the entropy of the model:*

$$\rho_j^P s(\mathcal{T}_j^P, e_j^P) - \rho_j^n s(1/\rho_j^n, e_j^n) + \frac{\Delta t}{\Delta x_j} (2q_{j+1/2}^n - 2q_{j-1/2}^n) \geq 0, \quad (39)$$

with $q_{i+1/2}^n = q_\Delta(\mathbf{U}_j^n, \mathbf{U}_{j+1}^n)$ where q_Δ is consistent with 0 as $\Delta t, \Delta x_j \rightarrow 0$.

Proof. By construction of the approximate Riemann solver $\mathbf{U}_{\text{RP}}^\theta, \Pi_{\text{RP}}^\theta, \mathcal{T}_{\text{RP}}^\theta$ in D, one can see that (37) is preserved by the pressure update (32a), which proves 1. Assertion 2. is a direct consequence of the consistency in the integral sense with the hypothesis (38). The truncation error (34) yields 3. Finally the positivity of the internal energy and the entropy inequality of 4. are a direct consequence of the approximate Riemann solver properties of proposition D.2 and consistency in the integral sense [17]. \square

Remark 5.1. In order to ensure $\theta = O(M)$, we suggest the following formula:

$$\theta_{i+1/2} = \min \left(1, |u_{i+1/2}^*| / \min(c_i, c_{i+1}) \right) \quad (40)$$

note that in some cases, this choice can violate inequality (110). However, in practice we did not observe any case where it induced problematic behavior. Note that (110). can be manually enforced and corresponds to imposing a minimum value on θ .

Let us now turn to the properties of the advection discretization.

Proposition 5.2. The discretization (23) of the advection subsystem verifies the following properties.

1. The advection subsystem discretization (23) is well-balanced in the sense that it preserves discrete hydrostatic solutions defined by (37).
2. The truncation error of the scheme (23) is uniform with respect to M when $M \ll 1$.
3. Under the CFL conditions (24): \mathbf{U}_j^A is a positive linear combination of \mathbf{U}_{j-1}^n , \mathbf{U}_j^n and \mathbf{U}_{j+1}^n .
4. Under the CFL conditions (24): b_j^A is a convex combination of b_{j-1}^n , b_j^n and b_{j+1}^n for $b \in \{u, E, \mathcal{T}\}$.
5. Under the CFL conditions (24): if $e_j^n > 0$ for all $j \in \mathbb{Z}$ then $e_j^A > 0$ for all $j \in \mathbb{Z}$.
6. The discretization (32a) satisfies the following inequality that involves the entropy of the model:

$$\rho_j^A s(\mathcal{T}_j^A, e_j^A) - \rho_j^n s_j^n + \frac{\Delta t}{\Delta x_j} \left(2u_{j+1/2}^* \rho_{j+1/2}^n s_{j+1/2}^n - 2u_{j-1/2}^* \rho_{j-1/2}^n s_{j-1/2}^n \right) \geq 0. \quad (41)$$

Proof. The assertion 1. is a direct consequence of the null velocity assumed by the hydrostatic profile (37). The truncation error (35) yields 2. The advection scheme (23) can be recast into

$$\mathbf{U}_j^A = -2 \frac{\Delta t}{\Delta x_j} u_{j+1/2}^{*, -} \mathbf{U}_{j+1}^n + 2 \frac{\Delta t}{\Delta x_j} u_{j-1/2}^{*, +} \mathbf{U}_{j-1}^n + \left[1 - 2 \frac{\Delta t}{\Delta x_j} (u_{j+1/2}^{*, +} - u_{j-1/2}^{*, -}) \right] \mathbf{U}_j^n, \quad (42)$$

which proves 3. One can also write

$$\left(\frac{\mathbf{U}}{\rho} \right)_j^A = \lambda_j^{(+1)} \left(\frac{\mathbf{U}}{\rho} \right)_{j+1}^n + \lambda_j^{(0)} \left(\frac{\mathbf{U}}{\rho} \right)_j^n + \lambda_j^{(-1)} \left(\frac{\mathbf{U}}{\rho} \right)_{j-1}^n, \quad (43)$$

with

$$\lambda_j^{(+1)} = -2 \frac{\Delta t}{\Delta x_j} u_{j+1/2}^{*, -} \left(\frac{\rho_{j+1}^n}{\rho_j^A} \right), \quad \lambda_j^{(0)} = \left[1 - 2 \frac{\Delta t}{\Delta x_j} (u_{j+1/2}^{*, +} - u_{j-1/2}^{*, -}) \right] \left(\frac{\rho_j^n}{\rho_j^A} \right), \quad \lambda_j^{(-1)} = 2 \frac{\Delta t}{\Delta x_j} u_{j-1/2}^{*, +} \left(\frac{\rho_{j-1}^n}{\rho_j^A} \right). \quad (44)$$

By (42) we have that

$$\rho_j^A = -2 \frac{\Delta t}{\Delta x_j} u_{j+1/2}^{*, -} \rho_{j+1}^n + 2 \frac{\Delta t}{\Delta x_j} u_{j-1/2}^{*, +} \rho_{j-1}^n + \left[1 - 2 \frac{\Delta t}{\Delta x_j} (u_{j+1/2}^{*, +} - u_{j-1/2}^{*, -}) \right] \rho_j^n, \quad (45)$$

so that $\lambda_j^{(+1)} + \lambda_j^{(0)} + \lambda_j^{(-1)} = 1$, which proves that b_j^A is a convex combination of b_{j-1}^n , b_j^n and b_{j+1}^n for $b \in \{u, E\}$.

Let us now consider the case of \mathcal{T}^A . By (25) we have that

$$\mathcal{T}_j^A = \mathcal{T}_j^n \frac{\rho_j^n}{\rho_j^A} - 2 \frac{\Delta t}{\Delta x_j} u_{j+1/2}^{*, +} \frac{1}{\rho_j^A} - 2 \frac{\Delta t}{\Delta x_j} u_{j+1/2}^{*, -} \frac{1}{\rho_j^A} + 2 \frac{\Delta t}{\Delta x_j} u_{j-1/2}^{*, +} \frac{1}{\rho_j^A} + 2 \frac{\Delta t}{\Delta x_j} u_{j-1/2}^{*, -} \frac{1}{\rho_j^A}. \quad (46)$$

However, if one accounts for the fact that $\rho_i^n \mathcal{T}_i^n = 1$ for all $i \in \mathbb{Z}$, then we can write that

$$\begin{aligned} \mathcal{T}_j^A &= \mathcal{T}_j^n \frac{\rho_j^n}{\rho_j^A} - 2 \frac{\Delta t}{\Delta x_j} u_{j+1/2}^{*, +} \frac{\rho_j^n}{\rho_j^A} \mathcal{T}_j^n - 2 \frac{\Delta t}{\Delta x_j} u_{j+1/2}^{*, -} \frac{\rho_{j+1}^n}{\rho_j^A} \mathcal{T}_{j+1}^n + 2 \frac{\Delta t}{\Delta x_j} u_{j-1/2}^{*, +} \frac{\rho_{j-1}^n}{\rho_j^A} \mathcal{T}_{j-1}^n + 2 \frac{\Delta t}{\Delta x_j} u_{j-1/2}^{*, -} \frac{\rho_j^n}{\rho_j^A} \mathcal{T}_j^n \\ &= \lambda_j^{(+1)} \mathcal{T}_{j+1}^n + \lambda_j^{(-1)} \mathcal{T}_{j-1}^n + \lambda_j^{(0)} \mathcal{T}_j^n. \end{aligned} \quad (47)$$

$$= \lambda_j^{(+1)} \mathcal{T}_{j+1}^n + \lambda_j^{(-1)} \mathcal{T}_{j-1}^n + \lambda_j^{(0)} \mathcal{T}_j^n. \quad (48)$$

Consequently \mathcal{T}_j^A is also a convex combination of \mathcal{T}_{j-1}^n , \mathcal{T}_j^n and \mathcal{T}_{j+1}^n , which proves 4. For the statement 5., we consider the concave function K introduced in the proof of lemma A.2 and we have that $e_j^A = K(u_j^A, E_j^A)$. Thanks to the statement 4. we can thus write that

$$e_j^A = K\left(\sum_{k=0,\pm 1} \lambda_j^{(k)} u_{j+k}^n, \sum_{k=0,\pm 1} \lambda_j^{(k)} E_{j+k}^n\right) \geq \sum_{k=0,\pm 1} \lambda_j^{(k)} K(u_{j+k}^n, E_{j+k}^n) = \sum_{k=0,\pm 1} \lambda_j^{(k)} e_{j+k}^n > 0, \quad (49)$$

which proves statement 5.

Now using the lemma A.2 we have that

$$s(\mathcal{T}_j^A, e_j^A) = \mathcal{U}(\mathcal{T}_j^A, u_j^A, E_j^A) = \mathcal{U}\left(\sum_{k=0,\pm 1} \lambda_j^{(k)} \mathcal{T}_{j+k}^n, \sum_{k=0,\pm 1} \lambda_j^{(k)} u_{j+k}^n, \sum_{k=0,\pm 1} \lambda_j^{(k)} E_{j+k}^n\right) \quad (50)$$

$$\geq \sum_{k=0,\pm 1} \lambda_j^{(k)} \mathcal{U}(\mathcal{T}_{j+k}^n, u_{j+k}^n, E_{j+k}^n) = \sum_{k=0,\pm 1} \lambda_j^{(k)} s(\mathcal{T}_{j+k}^n, e_{j+k}^n). \quad (51)$$

This inequality also reads

$$s(\mathcal{T}_j^A, e_j^A) \geq s_j^n \frac{\rho_j^n}{\rho_j^A} - 2 \frac{\Delta t}{\Delta x_j} u_{j+1/2}^{*,+} \frac{\rho_j^n}{\rho_j^A} s_j^n - 2 \frac{\Delta t}{\Delta x_j} u_{j+1/2}^{*, -} \frac{\rho_{j+1}^n}{\rho_j^A} s_{j+1}^n + 2 \frac{\Delta t}{\Delta x_j} u_{j-1/2}^{*,+} \frac{\rho_{j-1}^n}{\rho_j^A} s_{j-1}^n + 2 \frac{\Delta t}{\Delta x_j} u_{j-1/2}^{*, -} \frac{\rho_j^n}{\rho_j^A} s_j^n. \quad (52)$$

If the CFL condition (24) is met then $\rho_j^A \geq 0$ and by multiplying (52) by ρ_j^A we get (41). \square

From propositions 5.1 and 5.2 we now deduce the proposition.

Proposition 5.3. *The full numerical (26) verifies the following properties.*

1. *In the case $S = 0$, the scheme (26) is conservative with respect to mass, momentum and total energy for any $\theta \in [0, 1]$.*
2. *The numerical scheme (26) is well-balanced in the sense that it preserves discrete hydrostatic solutions defined by (37) for any $\theta \in [0, 1]$.*
3. *If $\theta = O(M)$ (e.g. via (40)), the truncation error of the scheme (26) is uniform with respect to M when $M \ll 1$.*
4. *Suppose that a is chosen large enough so that (38) is verified and (110) is valid: under the CFL conditions (21) and (24):*
 - (a) *if $\rho_j^0 > 0$, the scheme (26) ensures that $\rho_j^n > 0$,*
 - (b) *the scheme (26) ensures that $\rho_j^n e_j^n > 0$,*
 - (c) *the scheme (26) satisfies a discrete entropy inequality*

$$\rho_j^{n+1} s(1/\rho_j^{n+1}, e_j^{n+1}) - \rho_j^n s(1/\rho_j^n, e_j^n) + \frac{\Delta t}{\Delta x_j} (Q_{j+1/2} - Q_{j-1/2}) \geq 0, \quad (53)$$

$$\text{with } Q_{j+1/2} = u_{j+1/2}^* \rho_{j+1/2}^n s_{j+1/2}^n + q_{j+1/2}^n.$$

Proof. 1., 2. and 3. are straightforward consequences of proposition 5.1 and 5.2. Let us suppose that $\rho_j^n > 0$, then $\rho_j^P = \rho_j^n > 0$ and $\rho_j^A > 0$ by 3) in proposition 5.2. We have then $\rho_j^{n+1} = (\rho_j^A + \rho_j^P)/2 > 0$, which proves 4a).

If Λ is the concave function defined in the proof of lemma A.3, we have that

$$\begin{aligned} (\rho e)_j^{n+1} &= (\rho E)_j^{n+1} - \frac{((\rho u)_j^{n+1})^2}{2\rho_j^{n+1}} = \Lambda(\rho_j^{n+1}, (\rho u)_j^{n+1}, (\rho E)_j^{n+1}) = \Lambda\left(\frac{\rho_j^A + \rho_j^P}{2}, \frac{(\rho u)_j^A + (\rho u)_j^P}{2}, \frac{(\rho E)_j^A + (\rho E)_j^P}{2}\right) \\ &\geq \frac{1}{2} \Lambda(\rho_j^A, (\rho u)_j^A, (\rho E)_j^A) + \frac{1}{2} \Lambda(\rho_j^P, (\rho u)_j^P, (\rho E)_j^P) = \frac{(\rho e)_j^A + (\rho e)_j^P}{2}. \end{aligned} \quad (54)$$

Thanks to the propositions 5.1 and 5.2 we deduce then that $(\rho e)_j^{n+1} > 0$.

We have

$$\begin{aligned}\rho_j^{n+1} s(1/\rho_j^{n+1}, e_j^{n+1}) &= \rho_j^{n+1} s\left(\frac{1}{\rho_j^{n+1}}, \frac{(\rho E)_j^{n+1}}{\rho_j^{n+1}} - \frac{1}{2} \left(\frac{(\rho u)_j^{n+1}}{\rho_j^{n+1}}\right)^2\right) = \eta(\rho_j^{n+1}, 1, (\rho u)_j^{n+1}, (\rho E)_j^{n+1}) \\ &= \eta(\rho_j^{n+1}, (\rho \mathcal{T})_j^{n+1}, (\rho u)_j^{n+1}, (\rho E)_j^{n+1}) = \eta\left(\sum_{k=A,P} \frac{\rho_j^k}{2}, \sum_{k=A,P} \frac{(\rho \mathcal{T})_j^k}{2}, \sum_{k=A,P} \frac{(\rho u)_j^k}{2}, \sum_{k=A,P} \frac{(\rho E)_j^k}{2}\right).\end{aligned}\quad (55)$$

Thanks to lemma A.3 we know that η is concave and thus we have

$$\rho_j^{n+1} s(1/\rho_j^{n+1}, e_j^{n+1}) \geq \sum_{k=A,P} \frac{1}{2} \eta(\rho_j^k, (\rho \mathcal{T})_j^k, (\rho u)_j^k, (\rho E)_j^k) = \sum_{k=A,P} \frac{1}{2} \rho_j^k s(\mathcal{T}_j^k, e_j^k). \quad (56)$$

Using (39) and (41), we get

$$\rho_j^{n+1} s(1/\rho_j^{n+1}, e_j^{n+1}) \geq \rho_j^n s(1/\rho_j^n, e_j^n) - \frac{\Delta t}{\Delta x_j} (q_{j+1/2}^n - q_{j-1/2}^n) - \frac{\Delta t}{\Delta x_j} (u_{j+1/2}^* \rho_{j+1/2}^n s_{j+1/2}^n - u_{j-1/2}^* \rho_{j-1/2}^n s_{j-1/2}^n), \quad (57)$$

which proves 4c). \square

6 Alternative Energy source term discretizations

In this section, we propose two alternative discretizations of the source term. Indeed, the formula (20d) allows to derive an entropy inequality but does not satisfy the two following properties:

1. It is not conservative with respect to the total mechanical energy $\mathcal{E} = E + \phi$,
2. The internal energy is impacted by the source term.

depending on the field of application, the user of the solver may prefer one of these alternative discretizations.

6.1 Conservation of the mechanical energy

The first alternative allows the conservation of the total mechanical energy up to machine precision. It is really easy to derive. First, note that the energy equation (1) rewrites for \mathcal{E} :

$$(\rho \mathcal{E})_t + (u(\rho \mathcal{E}) + pu)_x = 0$$

on which we can perform the following conservative discretization:

$$(\rho \mathcal{E})_j^{n+1} = (\rho \mathcal{E})_j^n - \frac{\Delta t}{\Delta x} \left(u_{j+1/2}^* (\rho \mathcal{E})_{j+1/2}^n + \Pi_{j+1/2}^{*,\theta} u_{j+1/2}^* - u_{j-1/2}^* (\rho \mathcal{E})_{j-1/2}^n - \Pi_{j-1/2}^{*,\theta} u_{j-1/2}^* \right) \quad (58)$$

the method can be directly implemented taking \mathcal{E} as a variable and is conservative with respect to \mathcal{E} by construction. It also corresponds to a specific discretization of the energy source term when using the total energy E as a variable.

Proposition 6.1. *The discretization:*

$$\{\rho u \partial_x \phi\} = \frac{1}{\Delta x} \left(u_{j+1/2}^{*,-} \rho_{j+1}^n (\phi_{j+1} - \phi_j) + u_{j-1/2}^{*,+} \rho_{j-1}^n (\phi_j - \phi_{j-1}) \right). \quad (59)$$

instead of (20d) corresponds to the update (58) and is thus conservative.

Proof. We perform a straightforward expansion of $\rho \mathcal{E}$ in (58):

$$\begin{aligned}(\rho E)_j^{n+1} + \rho_j^{n+1} \phi_j &= (\rho E)_j^n + \rho_j^n \phi_j - \frac{\Delta t}{\Delta x} \left(u_{j+1/2}^* (\rho E)_{j+1/2}^n + p_{j+1/2}^{*,\theta} u_{j+1/2}^* - u_{j-1/2}^* (\rho E)_{j-1/2}^n - p_{j-1/2}^{*,\theta} u_{j-1/2}^* \right) \\ &\quad - \frac{\Delta t}{\Delta x} \left(u_{j+1/2}^* (\rho \phi)_{j+1/2}^n - u_{j-1/2}^* (\rho \phi)_{j-1/2}^n \right). \\ (\rho E)_j^{n+1} &= (\rho E)_j^n - \frac{\Delta t}{\Delta x} \left(u_{j+1/2}^* (\rho E)_{j+1/2}^n + p_{j+1/2}^{*,\theta} u_{j+1/2}^* - u_{j-1/2}^* (\rho E)_{j-1/2}^n - p_{j-1/2}^{*,\theta} u_{j-1/2}^* \right) \\ &\quad - \Delta t \{\rho u \partial_x \phi\}_j^n,\end{aligned}$$

where

$$\begin{aligned}\{\rho u \partial_x \phi\}_j^n &= \frac{1}{\Delta x} \left(u_{j+1/2}^* \rho_{j+1/2}^n (\phi_{j+1/2} - \phi_j) + u_{j-1/2}^* \rho_{j-1/2}^n (\phi_j - \phi_{j-1/2}) \right) \\ &= \frac{1}{\Delta x} \left(u_{j+1/2}^{*, -} \rho_{j+1}^n (\phi_{j+1} - \phi_j) + u_{j-1/2}^{*, +} \rho_{j-1}^n (\phi_j - \phi_{j-1}) \right).\end{aligned}$$

□

for which we do not have a proof of entropy inequality.

6.2 Unmodified internal energy

The second alternative is motivated by the fact that the gravitational source terms should not modify the internal energy i.e., if we note $\mathbf{U}^{n+1, '}$:

$$\begin{cases} \rho_j^{n+1, '} = \rho_j^{n+1} \\ (\rho u)_j^{n+1, '} : (\rho u)_j^n - \frac{\Delta t}{\Delta x} \left(u_{j+1/2}^* (\rho u)_{j+1/2}^n + \Pi_{j+1/2}^{*, \theta} - u_{j-1/2}^* (\rho u)_{j-1/2}^n - \Pi_{j-1/2}^{*, \theta} \right) \\ (\rho E)_j^{n+1, '} = (\rho E)_j^n - \frac{\Delta t}{\Delta x} \left(u_{j+1/2}^* (\rho E)_{j+1/2}^n + \Pi_{j+1/2}^{*, \theta} u_{j+1/2}^* - u_{j-1/2}^* (\rho E)_{j-1/2}^n - \Pi_{j-1/2}^{*, \theta} u_{j-1/2}^* \right) \end{cases} \quad (60)$$

i.e. the updated state without source terms, then the update (10a) gives $e^{n+1, '} \neq e^{n+1}$. If we keep $\{\rho \partial_x \phi\}$ from (20d) unchanged in order to preserve the well-balanced property, one can compute that $e^{n+1, '} = e^{n+1}$ implies

$$\begin{aligned} \{\rho u \partial_x \phi\}_j^n &= \{u\}_j^n \{\rho \partial_x \phi\}_j^n \\ \text{where } \{u\}_j^n &= u_j^{n+1, '} - \frac{1}{2} \frac{\Delta t}{\rho_j^{n+1}} \{\rho \partial_x \phi\}_j^n \end{aligned} \quad (61)$$

Proposition 6.2. *The scheme equipped with the internal energy preserving source term is endowed with a discrete entropy inequality.*

Proof. The scheme for the homogenous set of equations is endowed with a discrete entropy inequality (see [27] or consider the special case $\partial_x \phi = 0$ in this paper). Thus, $s(1/\rho_j^{n+1, '}, e_j^{n+1, '})$ follows an entropy inequality. Moreover, $1/\rho_j^{n+1, '} = 1/\rho_j^{n+1}$ and $e_j^{n+1, '} = e_j^{n+1}$ by design of the source term, hence the desired result. □

7 Numerical experiment

All the following tests are performed with a perfect gas EOS $p = \rho e(\gamma - 1)$ with $\gamma = 1.4$ or 1.6 .

7.1 The Sod shock tube

We considere here the classic Sod shock tube test case [40]. We set $\gamma = 1.4$ and the initial conditions are set to:

$$(\rho, u, p) = \begin{cases} (1, 0, 1) & \text{if } x < 0.5, \\ (0.125, 0, 0.1) & \text{if } x > 0.5. \end{cases}$$

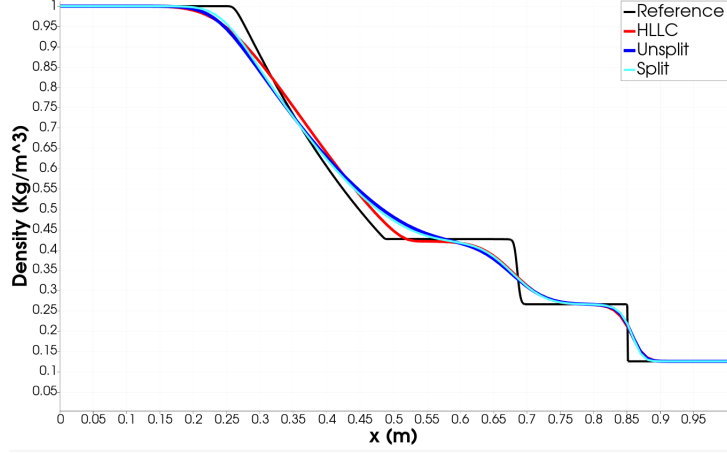


Figure 1: Resolution of the Sod shock tube problem with 3 different methods: Coarse HLLC, Unsplit and Split schemes. Resolution: 100 cells, $CFL = 0.99$. The Reference was generated with HLLC and 10000 cells.

Figure 1 shows the profile obtained at $t = 0.2s$ with three different methods: HLLC, Unsplit and Split along with a reference solution. The HLLC solver provides the sharpest resolution of the shock and the discontinuity of all three methods. The interest of this test in our study is to show that our solver is stable when dealing with shocks and to ensure that it propagates the different waves at the right speed. Both requirements are clearly satisfied. No spurious oscillation is observed and the center of the waves matches on all 4 curves. The difference between the Split and Unsplit method is hardly visible.

7.2 2D Riemann problem

We now consider the 2D Riemann problem introduced in [41] with $\gamma = 1.4$. This tests involves the evolution of 4 states that are put in contact in a squared box of side length 1. The initial data is the following:

$$(\rho, u, v, p) = \begin{cases} (0.138, 1.206, 1.206, 0.029) & \text{if } x < 0.8 \text{ } y < 0.8 \text{ (bottom left)} \\ (0.5323, 0.0, 1.206, 0.3) & \text{if } x > 0.8 \text{ } y < 0.8 \text{ (bottom right)} \\ (0.5323, 1.206, 0.0, 0.3) & \text{if } x < 0.8 \text{ } y > 0.8 \text{ (top left)} \\ (1.5, 0.0, 0.0, 1.5) & \text{if } x > 0.8 \text{ } y > 0.8 \text{ (top right)} \end{cases}$$

The results are usually displayed at time $t = 0.8$. This test challenges the ability of the scheme to deal with two-dimensional shocks propagation. It also measures the numerical dissipation as a complex feature appears in the middle of the domain.

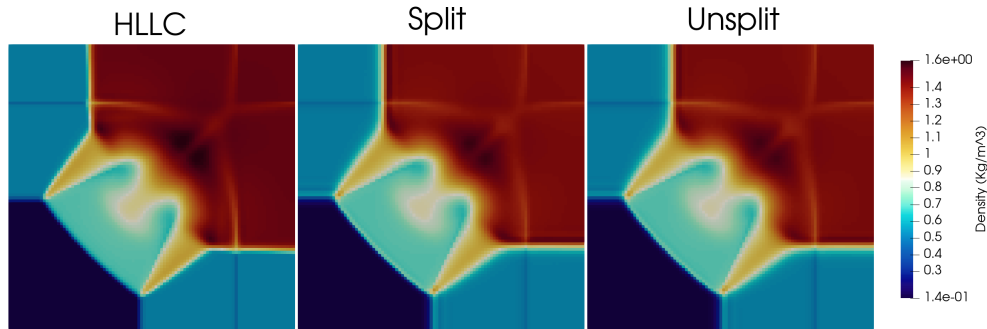


Figure 2: Resolution of the 2D Riemann problem with 3 different methods: HLLC, Unsplit and Split. Resolution: 100^2 cells with $CFL = 0.99$

Figure 2 shows that the three methods essentially provide the same final density map since this test does not involve a low Mach flow. However, it demonstrates the stability of the method in a two dimensional context.

7.3 Einfeldt's Strong Rarefaction

We test our numerical method against the Einfeldt's Strong Rarefaction test [42] in order to challenge the robustness of the solver when dealing with low densities or pressures. The initial conditions are

$$(\rho, u, p) = \begin{cases} (1, -2, 0.4), & \text{if } x < 0.5, \\ (1, 2, 0.4), & \text{if } x > 0.5, \end{cases}$$

and we use $\gamma = 1.4$.

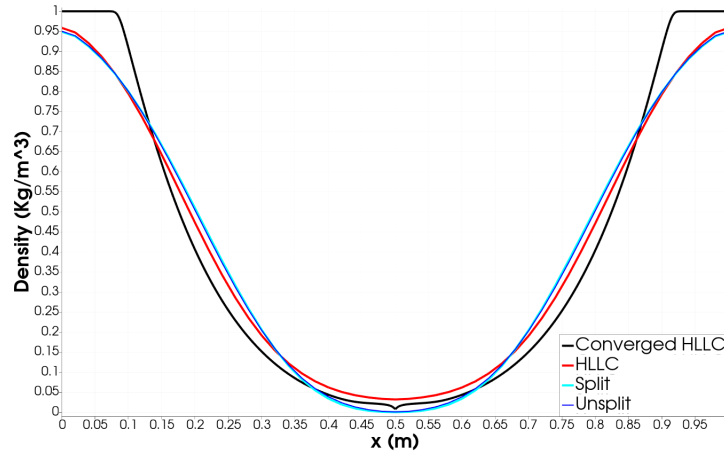


Figure 3: Resolution of the Einfeldt's Strong Rarefaction problem with 3 different methods: HLLC, Unsplit and Split. Resolution: 50 cells cells with $CFL = 0.99$. The reference solution has been generated with the HLLC scheme over a 10000-cell grid.

Figure 3 shows that all three methods are robust to the strong rarefaction, providing very similar results. In particular the numerical scheme does not exhibit entropy-related issue with the apparition of nonphysical shocks in the intermediate states of the strong rarefaction.

7.4 Atmosphere at rest

The atmosphere at rest test case is a simple column of atmosphere at equilibrium. The test allows us to measure the ability of a given scheme to preserve (8). We suppose that $\gamma = 5/3$ and we initialize the simulation with a linear temperature profile, according to (37) with the following parameters:

$$\phi = -gy = y, \quad e_{gnd} = 3.78565, \quad \rho_{gnd} = 1, \quad \nabla e = -1.2,$$

We copy the profile column by column on the $[0, 2] \times [0, 1]$ rectangle discretized over a 40×80 -cell grid. Then we let the solver evolve the profile for $t \in [0, 100s]$ and check if spurious velocities are created.

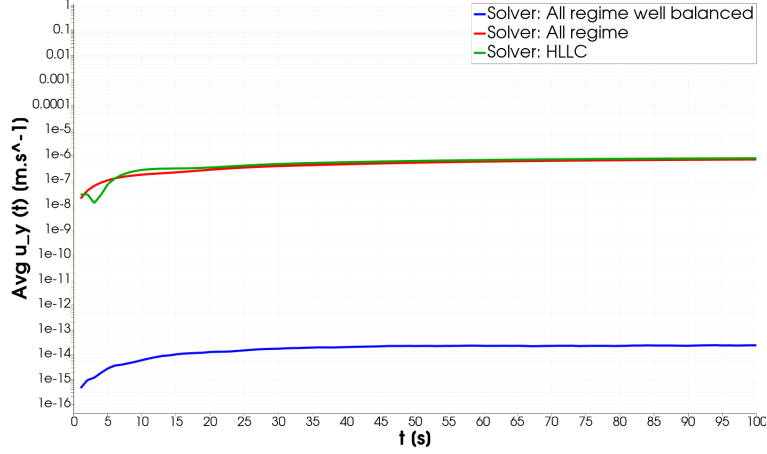


Figure 4: Comparison of the Split well-balanced method (blue), Split method with well-balanced correction turned off (red) and HLLC (green) on the atmosphere at rest test case. The quantity plotted is the average vertical velocity as a function of time $u_y^{avg}(t) = \frac{1}{|\Omega|} \int_{(x,y) \in \Omega} |u_y(x,y,t)| dx dy$ where $|\Omega|$ is the surface area of the domain.

Figure 4 compares the average vertical velocity as a function of time in the whole computational domain. The Split method is able to preserve this value around the machine round-off error (about 10^{-14} – 10^{-15} [m/s]). HLLC and Split method without well-balanced correction (i.e. using (20b)) immediately creates a vertical velocity of magnitude 10^{-7} that is not negligible and could ultimately break the macroscopic equilibrium. The well-balanced correction allows to preserve the hydrostatic equilibrium at machine precision while the other methods fail to do so.

7.5 Rayleigh-Taylor instability

The Rayleigh-Taylor test case with the rectangular computational domain $[L_x/2, L_x/2] \times [-L_y/2, L_y/2]$ where two perfect gases with $\gamma = 5/3$ with different densities are superposed at equilibrium. The denser fluid lies on top of the lighter, so that the configuration unstable. We impose a constant gravity field and add a small, single mode velocity perturbation to break the equilibrium by imposing:

$$g = -0.1, \quad (62a)$$

$$\phi(x, y) = -gy, \quad (62b)$$

$$\rho(x, y) = \begin{cases} 1 & \text{for } y < 0, \\ 2 & \text{for } y \geq 0, \end{cases} \quad (62c)$$

$$p(x, y) = \rho gy = -\rho\phi, \quad (62d)$$

$$u(x, y) = 0, \quad (62e)$$

$$v(x, y) = \frac{C}{4} \left(1 + \cos\left(\frac{2\pi x}{L_x}\right) \right) \left(1 + \cos\left(\frac{2\pi y}{L_y}\right) \right), \quad (62f)$$

with a the magnitude of the velocity perturbation $C = 0.01$ and $(L_x, L_y) = (0.5, 1.5)$. We now compare how the different methods behave:

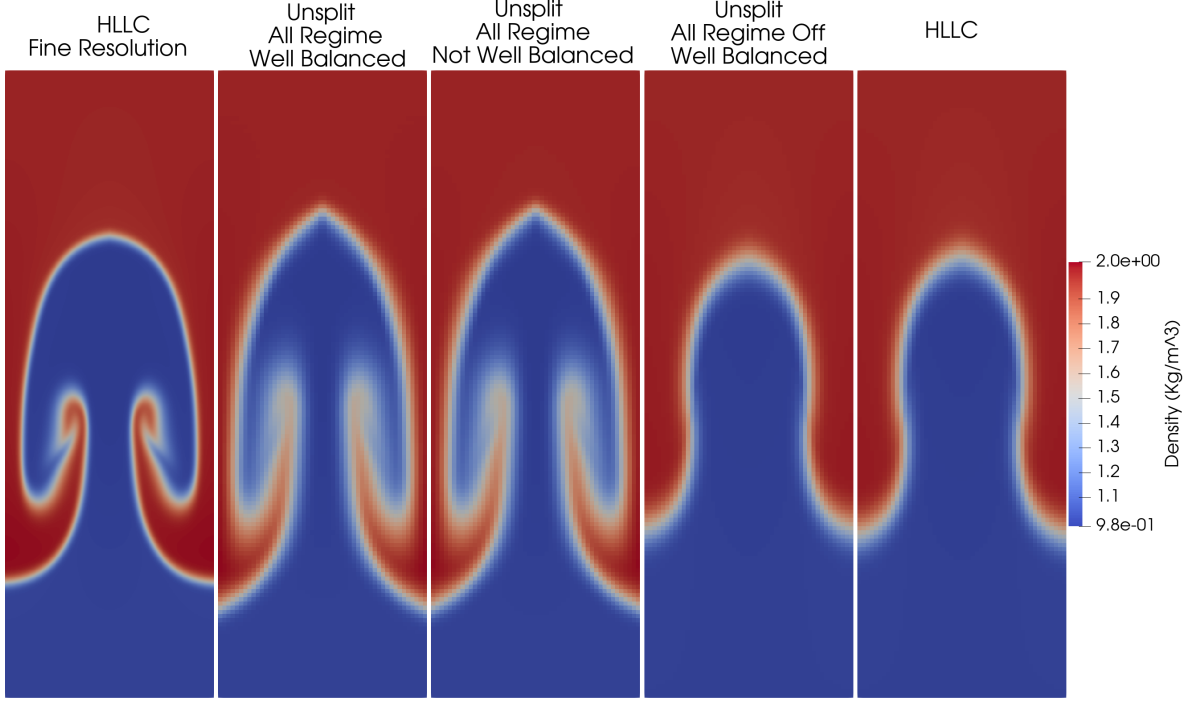


Figure 5: Several resolutions of the Rayleigh-Taylor instability. The coarse grid has a resolution of 50×150 , the fine grid is 200×600 , both with $CFL = 0.9$. Each rectangle corresponds to a different simulation. From left to right: fine HLLC, coarse Unsplit method, Unsplit not well-balanced, unsplit not well-balanced not all-regime, HLLC. Gravity is negative along the y axis.

Figure 5 compares several methods a reference HLLC solution. The HLLC and Unsplit with no low-Mach correction are both presenting an important amount of numerical diffusion: they only show a single mode growth and no lateral arm is created. On the other hand, The Unsplit method with low-Mach correction is able to produce these arms. It shows that our new method is able to capture high frequency features of the flow with much lower resolution than the classic HLLC solver. This is due to the low-Mach nature of this test. With the All-regime not well-balanced panel, we see that the well-balanced correction does not affect the final aspect of the density map. Note however how the low-Mach correction does not fix the important amount of numerical diffusion around the density discontinuity between both layers. The transition length between the two phases is much smaller on the fine reference resolution than in every coarse cases.

7.6 The Gresho vortex

The Gresho vortex [43] is a configuration used to test numerical schemes in the low-Mach regime. It is a stationary vortex that can be parametrized by the maximum value of the Mach number M_a across the computational domain. Using polar coordinates (r, θ) , the initial condition reads:

$$\begin{aligned} \rho &= \rho_0 = 1, \gamma = 1.4, \\ (u_r, u_\theta) &= \begin{cases} (0, 5r) & 0 \leq r < 0.2, \\ (0, 2 - 5r) & 0.2 \leq r < 0.4, \\ (0, 0) & 0.4 \leq r, \end{cases} \\ p &= \begin{cases} p_0 + 12.5r^2, & 0 \leq r < 0.2, \\ p_0 + 12.5r^2 + 4 - 20r + 4 \ln(5r), & 0.2 \leq r < 0.4, \\ p_0 - 2 + 4 \ln 2, & 0.4 \leq r. \end{cases} \end{aligned} \quad (63)$$

where $p_0 = \frac{1}{\gamma M_a^2}$. For a given value of M_a , the vortex is initialized and evolved to $10^{-3}s$. Then, we compare the original velocity magnitude profile to the one obtained as the solution of (63) is stationary.

Figure 6 gives us the final velocity magnitude map for the Gresho vortex obtained with different simulations. The first row is obtained with HLLC, second row with the all-regime split method and third row with the all-regime Unsplit

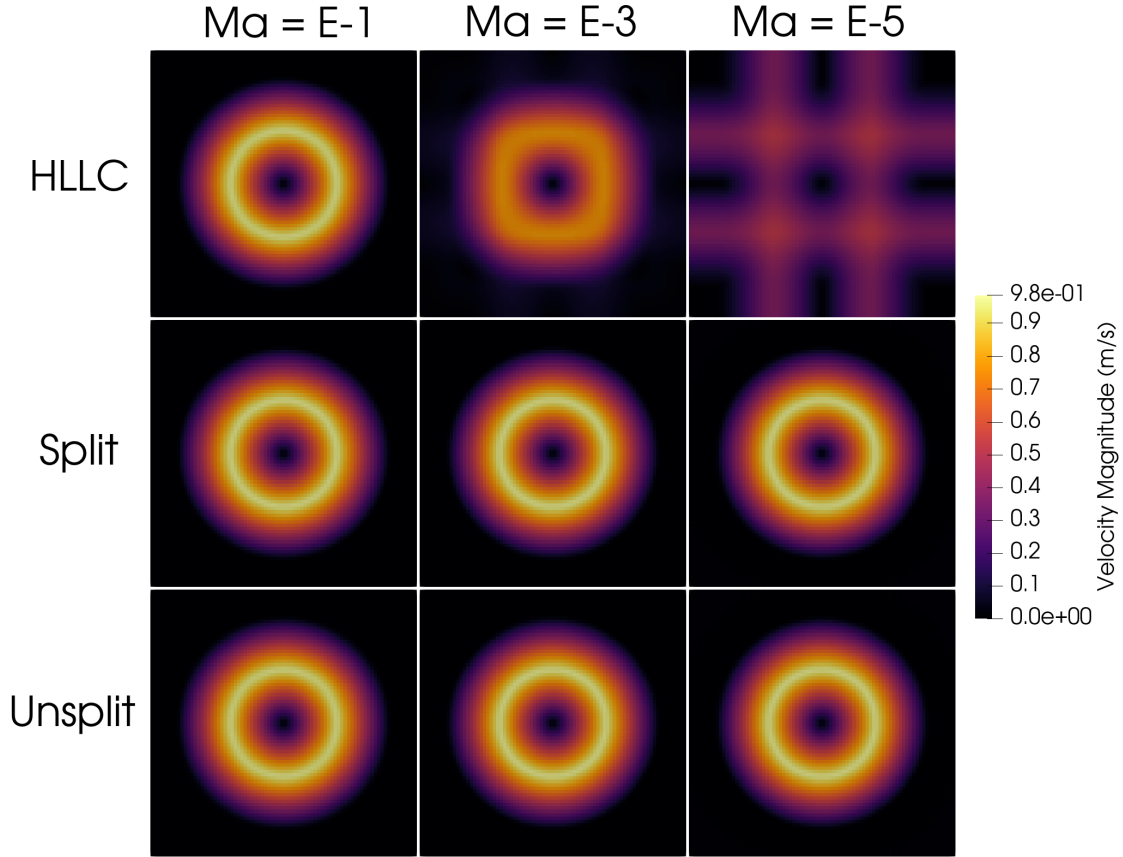


Figure 6: Comparison of the final velocity magnitude map for the Gresho vortex test case obtained with different solvers and Mach numbers. Each square is of size 1^2 and corresponds to a different simulation. The first row is obtained with HLLC, second row with the all-regime split method, third row with the all-regime Unsplit method. First column corresponds to $M = 10^{-1}$, second column to $M = 10^{-3}$ and third column to $M = 10^{-5}$. The resolution is 80^2 and $CFL = 0.4$.

method. The first column corresponds to $M = 10^{-1}$, the second column to $M = 10^{-3}$ and the third column to $M = 10^{-5}$. It is clear that the All regime solvers are able to preserve the structure of the vortex regardless of how small the Mach number is. However, the HLLC solver is not able to do so; the original vortex is deformed with $M = 10^{-3}$ and completely diffused away with $M = 10^{-5}$.

8 Conclusion

We proposed a finite volume method for the Euler equations with a source term induced by a potential. The numerical flux for the method is obtained by adding a flux for the pressure terms and a flux for the transport terms that are derived separately using the formalism introduced in [19]. We showed that this flux splitting method can be viewed as the result of a relaxation approximation that duplicates the initial set of variables in order to build a larger system where the pressure and the relaxation effects are almost decoupled. The fluid parameters are then obtained by taking the average of these duplicate flow variables.

Following the lines of [27], the analysis of the numerical scheme truncation error in the low Mach regime suggests to modify the numerical diffusion involved with the discretization of the pressure. This allows to derive a numerical scheme whose truncation error is uniform with respect to the Mach number. We then showed that under a CFL condition the scheme is positivity preserving for the mass and the internal energy. Moreover, under classic hypotheses in a non-vanishing Mach number regime the scheme verifies a discrete entropy inequality. The method is also well-balanced in the sense that it preserves hydrostatic equilibrium solutions.

The resulting numerical scheme is easy to implement and we have been able to successfully test its good stability and accuracy properties against one-dimensional and two-dimensional tests.

In future works we plan to investigate extensions to high-order methods and an implicit version of the solver for the acoustic flux in order to prevent the severe CFL limitations imposed by the sound velocity in the low Mach regime.

Acknowledgment

Pascal Tremblin acknowledges supports by the Euro-pean Research Council under Grant Agreement ATMO 757858

References

- [1] F. Liu, I. Jennions, and A. Jameson. Computation of turbomachinery flow by a convective-upwind-split-pressure (CUSP) scheme. In *36th AIAA Aerospace Sciences Meeting and Exhibit*, Reno,NV,U.S.A., 1998.
- [2] D. Darracq, S. Champagneux, and A. Corjon. Time-accurate fluid-structure coupling for turbulent flows. In C.-H. Bruneau, editor, *Sixteenth International Conference on Numerical Methods in Fluid Dynamics*, volume 515, pages pp. 31–36. Springer Berlin Heidelberg, 1998.
- [3] S. Evje and K. K. Fjelde. Hybrid flux-splitting schemes for a two-phase flow model. *Journal of Computational Physics*, 175(2):pp. 674–701, 2002.
- [4] H. Paillère, C. Corre, and J.R. García Cascales. On the extension of the AUSM+ scheme to compressible two-fluid models. *Computers & Fluids*, 32(6):pp. 891–916, 2003.
- [5] J.R. García-Cascales and H. Paillère. Application of AUSM schemes to multi-dimensional compressible two-phase flow problems. *Nuclear Engineering and Design*, 236(12):pp. 1225–1239, 2006.
- [6] J. L. Steger and R.F. Warming. Flux vector splitting of the inviscid gas dynamic equations with application to finite-difference methods. *Journal of Computational Physics*, 40(2):pp. 263–293, 1981.
- [7] G-C. Zha and E. Bilgen. Numerical solutions of Euler equations by using a new flux vector splitting scheme. *International Journal for Numerical Methods in Fluids*, 17(2):pp. 115–144, 1993.
- [8] M.-S. Liou and C. J. Steffen. A new flux splitting scheme. *Journal of Computational Physics*, 107(1):pp. 23–39, 1993.
- [9] A. Jameson. Analysis and design of numerical scheme for gas dynamics, 2: artificial diffusion and discrete shock structure. *International Journal of Computational Fluid Dynamics*, 5(1-2):pp. 1–38, 1995.
- [10] M.-S. Liou. Recent progress and applications of AUSM+. In *Sixteenth International Conference on Numerical Methods in Fluid Dynamics*, pages pp. 302–307. Springer Berlin Heidelberg, 1998.
- [11] M.-S. Liou. A sequel to AUSM, Part II: AUSM+-up for all speeds. *Journal of Computational Physics*, 214(1):pp. 137–170, 2006.
- [12] M.-S. Liou. A Sequel to AUSM: AUSM+. *Journal of Computational Physics*, 129(2):pp. 364–382, 1996.
- [13] F. Bouchut. Entropy satisfying flux vector splittings and kinetic BGK models. *Numerische Mathematik*, 94(4):pp. 623–672, 2003.
- [14] E. F. Toro and M. E. Vázquez-Cendón. Flux splitting schemes for the Euler equations. *Computers and Fluids*, 70:pp. 1–12, 2012.
- [15] J. M. Greenberg, A. Y. LeRoux, R. Baraille, and A. Noussair. Analysis and approximation of conservation laws with source terms. *SIAM Journal on Numerical Analysis*, 34(5):pp. 1980–2007, 1997.
- [16] L. Gosse. A well-balanced flux-vector splitting scheme designed for hyperbolic systems of conservation laws with source terms. *Computers & Mathematics with Applications*, 39(9-10):pp. 135–159, 2000.
- [17] F. Bouchut. *Nonlinear stability of finite volume methods for hyperbolic conservation laws and well-balanced schemes for sources*. Frontiers in Mathematics. Birkhäuser, Basel Berlin, 2004.
- [18] P. Chandrashekar and C. Klingenberg. A second order well-balanced finite volume scheme for Euler equations with gravity. *SIAM Journal on Scientific Computing*, 37:pp. B382–B402, 2015.
- [19] C. Chalons, P. Kestener, S. Kokh, and M. Stauffert. A large time-step and well-balanced Lagrange-projection type scheme for the shallow-water equations. *arXiv preprint arXiv:1604.01738*, 2016.
- [20] J. P. Berberich, P. Chandrashekar, and C. Klingenberg. High order well-balanced finite volume methods for multi-dimensional systems of hyperbolic balance laws. *Computers and Fluids*, 219:pp. 104858, 2021.

- [21] S. M. Deshpande, N. Balakrishnan, and S. V. Raghurama Rao. PVU and wave-particle splitting schemes for Euler equations of gas dynamics. *Sadhana*, 19(6):pp. 1027–1054, 1994.
- [22] K. Borah, G. Natarajan, and A. K. Dass. A novel second-order flux splitting for ideal magnetohydrodynamics. *Journal of Computational Physics*, 313:pp. 159–180, 2016.
- [23] R. Baraille, G. Bourdin, F. Dubois, and A.Y. Roux. Une version à pas fractionnaires du schéma de Godunov pour l’hydrodynamique. *C. R. Acad. Sci. Paris*, 314:pp. 147–152, 1992.
- [24] T. Buffard and J.M. Hérard. A conservative fractional step method to solve non-isentropic Euler equations. *Computer Methods in Applied Mechanics and Engineering*, 144(3-4):pp. 199–225, 1997.
- [25] C. Chalons, F. Coquel, S. Kokh, and N. Spillane. Large time-step numerical scheme for the seven-equation model of compressible two-phase flows. In J. Fořt, J. Fürst, J. Halama, R. Herbin, and F. Hubert, editors, *Finite Volumes for Complex Applications VI: Problems & Perspectives*, volume 4, pages pp. 225–233. Springer Berlin Heidelberg, Berlin, Heidelberg, 2011.
- [26] F. Coquel, J.-M. Hérard, and K. Saleh. A splitting method for the isentropic Baer-Nunziato two-phase flow model. *ESAIM: Proceedings*, 38:pp. 241–256, 2012.
- [27] C. Chalons, M. Girardin, and S. Kokh. An all-regime Lagrange-projection-like scheme for the gas dynamics equations on unstructured meshes. *Communications in Computational Physics*, 20(1):188–233, July 2016.
- [28] C. Chalons, M. Girardin, and S. Kokh. An all-regime Lagrange-projection like scheme for 2D homogeneous models for two-phase flows on unstructured meshes. *Journal of Computational Physics*, 335, 2017.
- [29] T. Padioleau, P. Tremblin, E. Audit, P. Kestener, and S. Kokh. A high-performance and portable all-Mach regime flow solver code with well-balanced gravity. application to compressible convection. *The Astrophysical Journal*, 875(2):p. 128, 2019.
- [30] H. Weyl. Shock waves in arbitrary fluids. *Comm. Pure Appl. Math.*, 2(2-3):pp. 103–122, 1949.
- [31] H.B. Callen. *Thermodynamics and an introduction to thermostatics*. John Wiley & sons, 1985.
- [32] J. Smoller. *Shock waves and reaction diffusion equations*. Springer Verlag, 1983.
- [33] R. J. LeVeque. *Nonlinear conservation laws and finite volume methods*, pages 1–159. Springer Berlin Heidelberg, 1998.
- [34] E. Godwleski and P.-A. Raviart. *Hyperbolic Systems of Conservation Laws*. Ellipse, 1990.
- [35] D. Serre. *Systems of Conservation Laws*, volume 1. Cambridge University Press, 1999.
- [36] B. Després. Inégalité entropique pour un solveur conservatif du système de la dynamique des gaz en coordonnées de Lagrange. *Comptes Rendus de l’Académie des Sciences - Series I - Mathematics*, 324(11):pp. 1301–1306, 1997.
- [37] I. Suliciu. On the thermodynamics of rate-type fluids and phase transitions. I. rate-type fluids. *International Journal of Engineering Science*, 36(9):pp. 921–947, 1998.
- [38] C. Chalons and J.-F. Coulombel. Relaxation approximation of the Euler equations. *J. Math. Anal. Appl.*, 348(2):pp. 872–893, 2008.
- [39] F. Coquel, E. Godlewski, and N. Seguin. Relaxation of fluid systems. *Mathematical Models and Methods in Applied Sciences*, 22(08):pp. 1250014, 2012.
- [40] G. A. Sod. A survey of several finite difference methods for systems of nonlinear hyperbolic conservation laws. *Journal of Computational Physics*, 27(1):pp. 1–31, 1978.
- [41] C. W. Schulz-Rinne, J. P. Collins, and H. M. Glaz. Numerical solution of the Riemann problem for two-dimensional gas dynamics. *SIAM J. Sci. Comput.*, 14(6):pp. 1394–1414, 1993.
- [42] B. Einfeldt, C. D. Munz, P. L. Roe, and B. Sjögren. On Godunov-type methods near low densities. *Journal of Computational Physics*, 92(2):pp. 273–295, 1991.
- [43] P. M. Gresho and S. T. Chan. On the theory of semi-implicit projection methods for viscous incompressible flow and its implementation via a finite element method that also introduces a nearly consistent mass matrix. Part 2: Implementation. *Int. J. Numer. Meth. Fluids*, 11(5):pp. 621–659, 1990.
- [44] E. Godwleski and P.-A. Raviart. *Numerical Approximation of Hyperbolic Systems of Conservation Laws*. Springer New York, 2021.

A A few classic convexity properties

We recall hereafter a few classic convexity/concavity properties related to admissible states, entropy and energy of our flow model that can be found in the literature (see for example [44]). We propose short self-contained proofs of these properties for the sake of completeness.

Lemma A.1. *We have the following properties.*

- (a) *The function $\Lambda : \mathbf{U} = (\rho, \rho u, \rho E) \in [0, +\infty) \times \mathbb{R} \times [0, +\infty) \mapsto \Lambda(\mathbf{U}) = (\rho E) - \frac{(\rho u)^2}{2\rho}$ is concave.*
(b) *Ω is convex.*

Proof. Let $\theta_1 = 1 - \theta_2 \in [0, 1]$ and $\mathbf{U}_k \in [0, +\infty) \times \mathbb{R} \times [0, +\infty)$ for $k = 1, 2$, we have

$$\Lambda\left(\sum_{k=1,2} \theta_k \mathbf{U}_k\right) - \sum_{k=1,2} \theta_k \Lambda(\mathbf{U}_k) = \sum_{k=1,2} \theta_k (\rho E)_k + \frac{\theta_1 \theta_2}{\sum_{k=1,2} \theta_k \rho_k} \left[(\rho u)_1 \sqrt{\frac{\rho_2}{\rho_1}} - (\rho u)_2 \sqrt{\frac{\rho_1}{\rho_2}} \right]^2 \geq 0, \quad (64)$$

which proves (a). For (b), consider again $\theta_1 = 1 - \theta_2 \in [0, 1]$ and $\mathbf{U}_k \in \Omega$, $k = 1, 2$. If we note $\mathbf{U} = \sum_{k=1,2} \theta_k \mathbf{U}_k$, then $\mathbf{U} \in \Omega$. Indeed, we have that $\sum_{k=1,2} \theta_k \rho_k \geq 0$, and as $\rho e = \Lambda(\mathbf{U}) \geq \sum_{k=1,2} \theta_k \Lambda(\mathbf{U}_k) = \sum_{k=1,2} \theta_k \rho_k e_k \geq 0$, where $e_k = E_k - (u_k^2)/2$. This implies that $e \geq 0$. \square

Lemma A.2. *The function $\mathcal{U} : (\mathcal{T}, u, E) \mapsto s\left(\mathcal{T}, E - \frac{u^2}{2}\right)$ is strictly concave.*

Proof. The function $K : (u, E) \mapsto E - u^2/2$ is strictly concave and we have $\mathcal{U}(\mathcal{T}, u, E) = s(\mathcal{T}, K(u, E))$. Consider $\lambda \in [0, 1]$ and let us note $\lambda = \lambda_1$ and $\lambda_2 = 1 - \lambda$. We have that

$$\mathcal{U}\left(\sum_{k=1,2} \lambda_k \mathcal{T}_k, \sum_{k=1,2} \lambda_k u_k, \sum_{k=1,2} \lambda_k E_k\right) - \sum_{k=1,2} \lambda_k \mathcal{U}(\mathcal{T}_k, u_k, E_k) \quad (65)$$

$$= s\left(\sum_{k=1,2} \mathcal{T}_k, K\left(\sum_{k=1,2} \lambda_k u_k, \sum_{k=1,2} \lambda_k E_k\right)\right) - \sum_{k=1,2} \lambda_k s(\mathcal{T}_k, K(u_k, E_k)) \quad (66)$$

$$= s\left(\sum_{k=1,2} \mathcal{T}_k, K\left(\sum_{k=1,2} \lambda_k u_k, \sum_{k=1,2} \lambda_k E_k\right)\right) - s\left(\sum_{k=1,2} \mathcal{T}_k, \sum_{k=1,2} \lambda_k K(u_k, E_k)\right) \\ + s\left(\sum_{k=1,2} \mathcal{T}_k, \sum_{k=1,2} \lambda_k K(u_k, E_k)\right) - \sum_{k=1,2} \lambda_k s(\mathcal{T}_k, K(u_k, E_k)). \quad (67)$$

As K is concave, we get that

$$K\left(\sum_{k=1,2} \lambda_k u_k, \sum_{k=1,2} \lambda_k E_k\right) \geq \sum_{k=1,2} \lambda_k K(u_k, E_k). \quad (68)$$

By (3) we know that $e' \mapsto s^{\text{EOS}}(\overline{\mathcal{T}}, e')$ is increasing so that

$$s\left(\sum_{k=1,2} \mathcal{T}_k, K\left(\sum_{k=1,2} \lambda_k u_k, \sum_{k=1,2} \lambda_k E_k\right)\right) - s\left(\sum_{k=1,2} \mathcal{T}_k, \sum_{k=1,2} \lambda_k K(u_k, E_k)\right) \geq 0. \quad (69)$$

We also know that s is concave therefore

$$s\left(\sum_{k=1,2} \mathcal{T}_k, \sum_{k=1,2} \lambda_k K(u_k, E_k)\right) - \sum_{k=1,2} \lambda_k s(\mathcal{T}_k, K(u_k, E_k)) \geq 0. \quad (70)$$

By replacing (69) and (70) into (67) we obtain that

$$\mathcal{U}\left(\sum_{k=1,2}\lambda_k\mathcal{T}_k,\sum_{k=1,2}\lambda_k u_k,\sum_{k=1,2}\lambda_k E_k\right)\geq\sum_{k=1,2}\lambda_k\mathcal{U}(\mathcal{T}_k,u_k,E_k). \quad (71)$$

□

Lemma A.3. *The function $\eta : (\rho, \rho\mathcal{T}, \rho u, \rho E) \mapsto \rho s\left(\frac{\rho\mathcal{T}}{\rho}, \frac{(\rho E)}{\rho} - \frac{(\rho u)^2}{2\rho^2}\right)$ is strictly concave.*

Proof. If we note again $\mathbf{U} = (\rho, \rho u, \rho E)$, by (6), we have

$$\eta(\rho, \rho\mathcal{T}, \rho u, \rho E) = \rho s\left(\frac{\rho\mathcal{T}}{\rho}, \frac{(\rho E)}{\rho} - \frac{(\rho u)^2}{2\rho^2}\right) = S\left(\rho, \rho\mathcal{T}, \rho E - \frac{(\rho u)^2}{2\rho}\right) = S(\rho, \rho\mathcal{T}, \Lambda(\mathbf{U})). \quad (72)$$

Now we consider $\mathbf{U}_k = (\rho_k, \rho_k u_k, \rho_k E_k) \in \Omega$ and $\mathcal{T}_k \geq 0$, $k = 1, 2$, we have

$$\begin{aligned} & \eta\left(\sum_{k=1,2}\theta_k\rho_k,\sum_{k=1,2}\theta_k\rho_k\mathcal{T}_k,\sum_{k=1,2}\theta_k\rho_k u_k,\sum_{k=1,2}\theta_k\rho_k E_k\right) - \sum_{k=1,2}\theta_k\eta(\rho_k,\rho_k\mathcal{T}_k,\rho_k u_k,\rho_k E_k) \\ &= S\left(\sum_{k=1,2}\theta_k\rho_k,\sum_{k=1,2}\theta_k\rho_k\mathcal{T}_k,\Lambda\left(\sum_{k=1,2}\theta_k\mathbf{U}_k\right)\right) - \sum_{k=1,2}\theta_k S(\rho_k,\rho_k\mathcal{T}_k,\Lambda(\mathbf{U}_k)) \\ &= S\left(\sum_{k=1,2}\theta_k\rho_k,\sum_{k=1,2}\theta_k\rho_k\mathcal{T}_k,\Lambda\left(\sum_{k=1,2}\theta_k\mathbf{U}_k\right)\right) - S\left(\sum_{k=1,2}\theta_k\rho_k,\sum_{k=1,2}\theta_k\rho_k\mathcal{T}_k,\sum_{k=1,2}\theta_k\Lambda(\mathbf{U}_k)\right) \\ & \quad + S\left(\sum_{k=1,2}\theta_k\rho_k,\sum_{k=1,2}\theta_k\rho_k\mathcal{T}_k,\sum_{k=1,2}\theta_k\Lambda(\mathbf{U}_k)\right) - \sum_{k=1,2}\theta_k S(\rho_k,\rho_k\mathcal{T}_k,\Lambda(\mathbf{U}_k)) \end{aligned} \quad (73)$$

As Λ is concave, we have $\Lambda\left(\sum_{k=1,2}\theta_k\mathbf{U}_k\right) \geq \sum_{k=1,2}\theta_k\Lambda(\mathbf{U}_k)$ and as $\mathcal{E}' \mapsto S(\bar{\rho}, \bar{\mathcal{T}}, \mathcal{E}')$ is increasing, we have

$$S\left(\sum_{k=1,2}\theta_k\rho_k,\sum_{k=1,2}\theta_k\rho_k\mathcal{T}_k,\Lambda\left(\sum_{k=1,2}\theta_k\mathbf{U}_k\right)\right) - S\left(\sum_{k=1,2}\theta_k\rho_k,\sum_{k=1,2}\theta_k\rho_k\mathcal{T}_k,\sum_{k=1,2}\theta_k\Lambda(\mathbf{U}_k)\right) \geq 0. \quad (74)$$

Using the fact that S is concave, we also get

$$S\left(\sum_{k=1,2}\theta_k\rho_k,\sum_{k=1,2}\theta_k\rho_k\mathcal{T}_k,\sum_{k=1,2}\theta_k\Lambda(\mathbf{U}_k)\right) - \sum_{k=1,2}\theta_k S(\rho_k,\rho_k\mathcal{T}_k,\Lambda(\mathbf{U}_k)) \geq 0. \quad (75)$$

Injecting (74) and (75) into (73) provides

$$\eta\left(\sum_{k=1,2}\theta_k\rho_k,\sum_{k=1,2}\theta_k\rho_k\mathcal{T}_k,\sum_{k=1,2}\theta_k\rho_k u_k,\sum_{k=1,2}\theta_k\rho_k E_k\right) \geq \sum_{k=1,2}\theta_k\eta(\rho_k,\rho_k\mathcal{T}_k,\rho_k u_k,\rho_k E_k). \quad (76)$$

□

B Eigenstructure of the off-equilibrium ($14_{\nu=0}$)

Let us first express the acoustic part of ($14_{\nu=0}$) using a change of variables: accounting for $e^P = E^P - (u^P)^2/2$, the evolution equations for E^P , for Π^P and \mathcal{T}^P in ($14_{\nu=0}$) yield

$$\partial_t(\rho^P e^P) + 2\Pi^P \partial_x u^P = 0, \quad 2\partial_x u^P = \partial_t(\rho^P \Pi^P / a^2). \quad (77)$$

We thus obtain the stationary equations

$$\partial_t\left[e^P - \frac{(\Pi^P)^2}{2a^2}\right] = 0, \quad \partial_t\left[\mathcal{T}^P + \frac{\Pi^P}{a^2}\right] = 0. \quad (78)$$

So now the acoustic subsystem ($14a_\nu = 0$) takes the simple form

$$\partial_t \phi = 0, \quad \partial_t \rho^P = 0, \quad \partial_t \left[e^P - \frac{(\Pi^P)^2}{2a^2} \right] = 0, \quad (79a)$$

$$\partial_t(\rho^P u^P) + 2\partial_x \Pi^P + 2\rho^P \partial_x \phi^P = 0, \quad \partial_t(\rho^P \Pi^P) + 2a^2 \partial_x u^P = 0, \quad \partial_t \left[\mathcal{T}^P + \frac{\Pi^P}{a^2} \right] = 0. \quad (79b)$$

We now turn to the advection part of ($14_\nu = 0$): the subsystem ($14b_\nu = 0$) takes the simple form

$$\partial_t \rho^A + \partial_x(2\rho^A u^P) = 0, \quad \partial_t \left[\rho^A \mathcal{T}^A - \frac{\rho^P \Pi^P}{a^2} \right] = 0, \quad \partial_t b^A + 2u^P \partial_x b^A = 0, \quad b^A \in \{u^A, E^A, \Pi^A\}. \quad (80)$$

Therefore if we set

$$\mathbf{W}^T = \left[u^P, \Pi^P, \rho^P, \phi, e^P - \frac{(\Pi^P)^2}{2a^2}, \mathcal{T}^P + \frac{\Pi^P}{a^2}, \rho^A \mathcal{T}^A - \frac{\rho^P \Pi^P}{a^2}, u^A, \Pi^A, E^A, \rho^A \right], \quad (81)$$

we can see that ($14_\nu = 0$) can be recast into the following quasilinear system

$$\partial_t \mathbf{W} + \mathbf{M}(\mathbf{W}) \partial_x \mathbf{W} = 0, \quad \mathbf{M}(\mathbf{W}) = \begin{bmatrix} 0 & \frac{2}{\rho^P} & 0 & 2 & 0 & 0 & 0 & 0 & 0 & 0 & 0 & 0 \\ \frac{2a^2}{\rho^P} & 0 & 0 & 0 & 0 & 0 & 0 & 0 & 0 & 0 & 0 & 0 \\ 0 & 0 & 0 & 0 & 0 & 0 & 0 & 0 & 0 & 0 & 0 & 0 \\ 0 & 0 & 0 & 0 & 0 & 0 & 0 & 0 & 0 & 0 & 0 & 0 \\ 0 & 0 & 0 & 0 & 0 & 0 & 0 & 0 & 0 & 0 & 0 & 0 \\ 0 & 0 & 0 & 0 & 0 & 0 & 0 & 0 & 0 & 0 & 0 & 0 \\ 0 & 0 & 0 & 0 & 0 & 0 & 0 & 0 & 0 & 0 & 0 & 0 \\ 0 & 0 & 0 & 0 & 0 & 0 & 0 & 2u^P & 0 & 0 & 0 & 0 \\ 0 & 0 & 0 & 0 & 0 & 0 & 0 & 0 & 2u^P & 0 & 0 & 0 \\ 0 & 0 & 0 & 0 & 0 & 0 & 0 & 0 & 0 & 2u^P & 0 & 0 \\ 2\rho^A & 0 & 0 & 0 & 0 & 0 & 0 & 0 & 0 & 0 & 2u^P & 0 \end{bmatrix}. \quad (82)$$

It is then straightforward to see that the eigenvalues of $\mathbf{M}(\mathbf{W})$ are $2u^P$ (with an algebraic multiplicity 4), 0 (with an algebraic multiplicity 5) and $\pm 2a/\rho^P$.

The eigenvectors $\left(\mathbf{r}_0^{(k)} \right)_{k=1,\dots,3}$, $\left(\mathbf{r}_{u^P}^{(k)} \right)_{k=1,\dots,4}$ and \mathbf{r}_\pm that are respectively associated with 0, $2u^P$ and $\pm 2a/\rho^P$ are

$$\mathbf{r}_0^{(1)} = [0, 0, 1, 0, 0, 0, 0, 0, 0, 0, 0, 0]^T, \quad \mathbf{r}_0^{(2)} = [0, -\rho^P, 0, 1, 0, 0, 0, 0, 0, 0, 0, 0]^T, \quad (83a)$$

$$\mathbf{r}_0^{(3)} = [0, 0, 0, 0, 1, 0, 0, 0, 0, 0, 0, 0]^T, \quad \mathbf{r}_0^{(4)} = [0, 0, 0, 0, 0, 1, 0, 0, 0, 0, 0, 0]^T \quad (83b)$$

$$\mathbf{r}_0^{(5)} = [0, 0, 0, 0, 0, 0, 1, 0, 0, 0, 0, 0]^T, \quad (83c)$$

$$\mathbf{r}_{u^P}^{(1)} = [0, 0, 0, 0, 0, 0, 0, 1, 0, 0, 0, 0]^T, \quad \mathbf{r}_{u^P}^{(2)} = [0, 0, 0, 0, 0, 0, 0, 0, 1, 0, 0, 0]^T, \quad (83d)$$

$$\mathbf{r}_{u^P}^{(3)} = [0, 0, 0, 0, 0, 0, 0, 0, 0, 1, 0, 0]^T, \quad \mathbf{r}_{u^P}^{(4)} = [0, 0, 0, 0, 0, 0, 0, 0, 0, 0, 1, 0]^T, \quad (83e)$$

$$\mathbf{r}_+ = \left[1, a, 0, 0, 0, 0, 0, 0, 0, 0, -\frac{\rho^A \rho^P}{\rho^P u^P - a} \right]^T, \quad \mathbf{r}_- = \left[1, -a, 0, 0, 0, 0, 0, 0, 0, 0, -\frac{\rho^A \rho^P}{\rho^P u^P + a} \right]^T, \quad (83f)$$

so that (82) is hyperbolic and only involves linearly degenerate fields.

C Approximate Riemann solver for the pressure subsystem

Let $\Delta x_L > 0$, $\Delta x_R > 0$ and suppose that $x \rightarrow \phi(x)$ is smooth. We consider \bar{x} and the following piecewise initial data

$$(\mathbf{U}^P, \Pi^P, \mathcal{T}^P, \phi)(x, t = 0) = \begin{cases} (\mathbf{U}_L^P, \Pi_L^P, \mathcal{T}_L^P, \phi_L) & \text{if } x \leq \bar{x}, \\ (\mathbf{U}_R^P, \Pi_R^P, \mathcal{T}_R^P, \phi_R) & \text{if } x > \bar{x}, \end{cases} \quad (84)$$

that verifies the equilibrium relations:

$$(\mathbf{U}_k^P, \Pi_k^P, \mathcal{T}_k^P, \phi_k) = \left[(\rho_k^P, \rho_k^P u_k^P, E_k^P)^T, p^{\text{EOS}} \left(\frac{1}{\rho_k^P}, e_k^P \right), \frac{1}{\rho_k^P}, \phi_k \right], \quad k = L, R, \quad (85)$$

with $\phi_L = \frac{1}{\Delta x_L} \int_{-\Delta x_L}^0 \phi(\bar{x} + x) dx$ and $\phi_R = \frac{1}{\Delta x_R} \int_0^{\Delta x_R} \phi(\bar{x} + x) dx$. We seek for a self-similar function $(\mathbf{U}_{RP}, \Pi_{RP}, \mathcal{T}_{RP}, \phi_{RP})$ composed of four constant states separated by three discontinuities as follows:

$$(\mathbf{U}_{RP}, \Pi_{RP}, \mathcal{T}_{RP}, \phi_{RP}) \left(\frac{x - \bar{x}}{t}; \mathbf{U}_L, \Pi_L, \mathcal{T}_L, \phi_L, \mathbf{U}_R, \Pi_R, \mathcal{T}_R, \phi_R \right) = \begin{cases} (\mathbf{U}_L, \Pi_L, \mathcal{T}_L, \Phi_L), & \text{if } \frac{x - \bar{x}}{t} \leq -\frac{2a}{\rho_L}, \\ (\mathbf{U}_L^*, \Pi_L^*, \mathcal{T}_L^*, \Phi_L), & \text{if } -\frac{2a}{\rho_L} < \frac{x - \bar{x}}{t} \leq 0, \\ (\mathbf{U}_R^*, \Pi_R^*, \mathcal{T}_R^*, \Phi_R), & \text{if } 0 < \frac{x - \bar{x}}{t} \leq \frac{2a}{\rho_R}, \\ (\mathbf{U}_R, \Pi_R, \mathcal{T}_R, \Phi_R), & \text{if } \frac{2a}{\rho_R} < \frac{x - \bar{x}}{t}, \end{cases} \quad (86)$$

where the intermediate states \mathbf{U}_k^* , Π_k^* and \mathcal{T}_k^* are required to satisfy the four following properties.

1. The approximate Riemann solver should be consistent in the integral sense with the pressure subsystem (17a): for Δt such that $\frac{2a}{\min(\rho_L, \rho_R)} \Delta t < \frac{1}{2} \min(\Delta x_L, \Delta x_R)$, we have

$$\begin{bmatrix} 2\mathbf{P}(\mathbf{U}_R) - 2\mathbf{P}(\mathbf{U}_L) \\ 2a^2(u_R^* - u_L^*) \\ -(2u_R^* - 2u_L^*) \end{bmatrix} = -\frac{2a}{\rho_L} \begin{bmatrix} \mathbf{U}_L^* - \mathbf{U}_L \\ (\rho\Pi)_L^* - (\rho\Pi)_L \\ (\rho\mathcal{T})_L^* - (\rho\mathcal{T})_L \end{bmatrix} + \frac{2a}{\rho_R} \begin{bmatrix} \mathbf{U}_R - \mathbf{U}_R^* \\ (\rho\Pi)_R - (\rho\Pi)_R^* \\ (\rho\mathcal{T})_R - (\rho\mathcal{T})_R^* \end{bmatrix} + (\Delta x_L + \Delta x_R) \{\mathbf{S}\}, \quad (87)$$

with $\{\mathbf{S}\}$ a function that is a consistent approximation of \mathbf{S} , that is to say:

$$\lim_{\substack{\Phi_L, \Phi_R \rightarrow \phi(\bar{x}) \\ \Delta x_L, \Delta x_R \rightarrow 0 \\ (\mathbf{U}_R, \Pi_R), (\mathbf{U}_L, \Pi_L) \rightarrow (\bar{\mathbf{U}}, p^{\text{EOS}}(\bar{\rho}, \bar{e}))}} \{\mathbf{S}\} = \mathbf{S}(\bar{\mathbf{U}}, \phi)(x = \bar{x}). \quad (88)$$

2. In the case $\phi_L = \phi_R$, the should be degenerate to an approximate Riemann for the homogeneous problem obtained with (17a) when $\mathbf{S} = \mathbf{0}$.
3. If \mathbf{U}_L and \mathbf{U}_R satisfy the following discrete version of the hydrostatic condition (8):

$$\Pi_R - \Pi_L = -\frac{\rho_L + \rho_R}{2}(\phi_R - \phi_L), \quad u_L = u_R = 0, \quad (89)$$

then $(\mathbf{U}_L^*, \Pi_L^*) = (\mathbf{U}_L, \Pi_L)$ and $(\mathbf{U}_R^*, \Pi_R^*) = (\mathbf{U}_R, \Pi_R)$.

Let us build the states $(\mathbf{U}_R^*, \Pi_R^*)$ and $(\mathbf{U}_L^*, \Pi_L^*)$ so that they verify the above properties. We note

$$\Pi_R^* - \Pi_L^* + \mathcal{M} = 0. \quad (90)$$

First, we impose that ρ_L^* and ρ_R^* are consistent with the exact solution of (17a) by setting $\rho_L^* = \rho_L$ and $\rho_R^* = \rho_R$. Then we also require that the Rankine-Hugoniot jump conditions obtained in the case $\mathbf{S} = \mathbf{0}$ are valid across the waves of velocity $-2a/\rho_L$ and $+2a/\rho_R$

$$\frac{2a}{\rho_L} \begin{bmatrix} \mathbf{U}_L^* - \mathbf{U}_L \\ (\rho\Pi)_L^* - (\rho\Pi)_L \\ (\rho\mathcal{T})_L^* - (\rho\mathcal{T})_L \end{bmatrix} + \begin{bmatrix} 2\mathbf{P}(\mathbf{U}_L^*) - 2\mathbf{P}(\mathbf{U}_L) \\ 2a^2 u_L^* - 2a^2 u_L \\ -2u_L^* + 2u_L \end{bmatrix} = 0, \quad -\frac{2a}{\rho_R} \begin{bmatrix} \mathbf{U}_R - \mathbf{U}_R^* \\ (\rho\Pi)_R - (\rho\Pi)_R^* \\ (\rho\mathcal{T})_R - (\rho\mathcal{T})_R^* \end{bmatrix} + \begin{bmatrix} 2\mathbf{P}(\mathbf{U}_R) - 2\mathbf{P}(\mathbf{U}_R^*) \\ 2a^2 u_R - 2a^2 u_R^* \\ -2u_R + 2u_R^* \end{bmatrix} = 0 \quad (91)$$

Finally, we postulate that the velocity is continuous across the stationary wave by setting

$$u_L^* = u_R^* = u^*, \quad (92)$$

and we also impose that $(\Pi u)_k^* = \Pi_k^* u_k^* = \Pi_k^* u^*$, $k = L, R$. Then, relations (87), (91), (90) yield

$$\rho_L^* = \rho_L, \quad \rho_R^* = \rho_R, \quad (93a)$$

$$E_L^* = E_L - \frac{1}{a} \left((\Pi^* + \frac{\mathcal{M}}{2}) u^* - \Pi_L u_L \right), \quad E_R^* = E_R + \frac{1}{a} \left((\Pi^* - \frac{\mathcal{M}}{2}) u^* - \Pi_R u_R \right), \quad (93b)$$

$$u^* = u_R^* = u_L^* = \frac{u_R + u_L}{2} - \frac{1}{2a} (\Pi_R - \Pi_L) - \frac{\mathcal{M}}{2a}, \quad \Pi^* = \frac{\Pi_R + \Pi_L}{2} - \frac{a}{2} (u_R - u_L), \quad (93c)$$

$$\Pi_L^* = \Pi^* + \frac{\mathcal{M}}{2}, \quad \Pi_R^* = \Pi^* - \frac{\mathcal{M}}{2}, \quad (93d)$$

$$\mathcal{T}_L^* = \frac{1}{\rho_L} + \frac{1}{a} (u^* - u_L), \quad \mathcal{T}_R^* = \frac{1}{\rho_R} - \frac{1}{a} (u^* - u_R), \quad (93e)$$

where the jump \mathcal{M} can be identified as

$$\mathcal{M} = \frac{\Delta x_L + \Delta x_R}{2} \{\rho \partial_x \phi\}, \quad \mathcal{M}u^* = \frac{\Delta x_L + \Delta x_R}{2} \{\rho u \partial_x \phi\}. \quad (94)$$

At this point, the functions $\{\rho \partial_x \phi\}$ and $\{\rho u \partial_x \phi\}$ are still yet to be specified. Let us consider the constraint 3: if it is satisfied then for a state that verifies (89) the jumps \mathcal{M} and $\mathcal{M}u^*$ necessarily take the value $\mathcal{M} = -(\Pi_R - \Pi_L)$ and $\mathcal{M}u^* = 0$. A simple choice that fulfills this requirement is

$$\{\rho \partial_x \phi\} = (\rho_L + \rho_R) \frac{\phi_R - \phi_L}{\Delta x_L + \Delta x_R}, \quad \{\rho u \partial_x \phi\} = (\rho_L + \rho_R) u^* \frac{\phi_R - \phi_L}{\Delta x_L + \Delta x_R}. \quad (95a)$$

Relations (93) and (95a) give a complete definition of the approximate Riemann solver (86). This solver yields a definition for the conservative numerical flux $\mathbf{P}_\Delta(\mathbf{U}_L, \Pi_L, \phi_L, \mathbf{U}_R, \Pi_R, \phi_R)$ and a source term discretization (located at the interface) $\mathbf{S}_\Delta(\mathbf{U}_L, \Pi_L, \phi_L, \mathbf{U}_R, \Pi_R, \phi_R)$ thanks to the consistency in the integral sense. We get

$$\mathbf{P}_\Delta(\mathbf{U}_L, \Pi_L, \phi_L, \mathbf{U}_R, \Pi_R, \phi_R) = \frac{\mathbf{P}(\mathbf{U}_R, \Pi_R) + \mathbf{P}(\mathbf{U}_L, \Pi_L)}{2} - \frac{a}{2\rho_L}(\mathbf{U}_L^* - \mathbf{U}_L) - \frac{a}{2\rho_R}(\mathbf{U}_R - \mathbf{U}_R^*), \quad (96a)$$

$$\mathbf{S}_\Delta(\mathbf{U}_L, \Pi_L, \phi_L, \mathbf{U}_R, \Pi_R, \phi_R) = [0, -\{\rho \partial_x \phi\}, -\{\rho u \partial_x \phi\}]^T, \quad (96b)$$

so that for two neighbouring states $(\mathbf{U}_j^n, \Pi_j^n, \phi_j)$ and $(\mathbf{U}_{j+1}^n, \Pi_{j+1}^n, \phi_{j+1})$ across the cell interface $j+1/2$ that separates the cell j and the cell $j+1$, the numerical conservative flux $\mathbf{P}_{j+1/2}$ is defined by

$$\mathbf{P}_{j+1/2} = \mathbf{P}_\Delta(\mathbf{U}_j^n, \Pi_j^n, \phi_j, \mathbf{U}_{j+1}^n, \Pi_{j+1}^n, \phi_{j+1}), \quad (97)$$

and the discrete source term \mathbf{S}_j within the cell j is given by

$$\mathbf{S}_j = \frac{\Delta x_{j+1/2}}{2\Delta x_j} \mathbf{S}_{j+1/2} + \frac{\Delta x_{j-1/2}}{2\Delta x_j} \mathbf{S}_{j-1/2}, \quad \mathbf{S}_{j+1/2} = \mathbf{S}_\Delta(\mathbf{U}_j^n, \Pi_j^n, \phi_j, \mathbf{U}_{j+1}^n, \Pi_{j+1}^n, \phi_{j+1}). \quad (98)$$

Let us now give some properties of the approximate Riemann solver. Let us note $e_k^* = E_k^* - (u_k^*)^2/2$, the following lemma is a direct consequence of (91) that exhibits a reminiscent property associated with the Riemann invariants associated of the system (17a) when $\mathbf{S} = 0$.

Lemma C.1.

$$e_k^* - \frac{(\Pi_k^*)^2}{2a^2} = e_k - \frac{(\Pi_k)^2}{2a^2}, \quad \mathcal{T}_k^* + \frac{\Pi_k^*}{a} = \mathcal{T}_k + \frac{\Pi_k}{a}, \quad k = L, R. \quad (99)$$

The following positivity result is a direct consequence of (93e).

Proposition C.1.

1. If a is chosen large enough then $\mathcal{T}_L^* > 0$ and $\mathcal{T}_R^* > 0$.
2. $\mathcal{T}_L^* > 0$ and $\mathcal{T}_R^* > 0$ is equivalent to $u_L - a\mathcal{T}_L = u_L - a/\rho_L < u^* < u_R + a\mathcal{T}_R = u_R + a/\rho_R$.

Following the lines of [19], we first prove two preliminary stability-related results. The differences from Lemma 1 of [19] are that the Riemann states we are dealing with here depends on the M terms and that the specific volume we use is \mathcal{T} instead of $\frac{1}{\rho}$ (that are different in the sub-system framework). However, the proof turns out to be almost identical.

Proposition C.2. Consider the intermediate states defined by (93).

and noting $s_k = s^{EOS}(\mathcal{T}_k, s_k)$, we have

$$e_k^* - e^{EOS}(\mathcal{T}_k^*, s_k) - \frac{(p^{EOS}(\mathcal{T}_k^*, s_k) - \Pi_k^*)^2}{2a^2} \geq 0, \quad (100)$$

with $e_k^* = E_k^* - \frac{u_k^{*2}}{2}$.

Proof. We only describe the case $k = R$. Consider the function:

$$\begin{aligned} \chi(\mathcal{T}) = e^{EOS}(\mathcal{T}, s_R) - \frac{p^{EOS}(\mathcal{T}, s_R)^2}{2a^2} - e^{EOS}(\mathcal{T}_R^*, s_R) + \frac{p^{EOS}(\mathcal{T}_R^*, s_R)^2}{2a^2} \\ + p^{EOS}(\mathcal{T}_R^*, s_R) \left(\mathcal{T} + \frac{p^{EOS}(\mathcal{T}, s_R)}{a^2} - \mathcal{T}_R^* - \frac{p^{EOS}(\mathcal{T}_R^*, s_R)}{a^2} \right). \end{aligned} \quad (101)$$

One can check that $\chi'(\mathcal{T}) = (p^{\text{EOS}}(\mathcal{T}_R^*, s_R) - p^{\text{EOS}}(\mathcal{T}, s_R)) (1 - \rho^2 c^2(\mathcal{T}, s_R) / a^2)$. We have $\partial_{\mathcal{T}} p < 0$ from 3, we also assume 38 which ensures $\text{sign}(\chi'(\mathcal{T})) = \text{sign}(p^{\text{EOS}}(\mathcal{T}_R^*, s_R) - p^{\text{EOS}}(\mathcal{T}, s_R))$. We have two different cases:

$$\begin{aligned} \mathcal{T}_R^* < \mathcal{T} < \mathcal{T}_R &\implies \chi'(\mathcal{T}) > 0 \implies \chi(\mathcal{T}_R^*) < \chi(\mathcal{T}) < \chi(\mathcal{T}_R). \\ \mathcal{T}_R^* > \mathcal{T} > \mathcal{T}_R &\implies \chi'(\mathcal{T}) < 0 \implies \chi(\mathcal{T}_R^*) < \chi(\mathcal{T}) < \chi(\mathcal{T}_R). \end{aligned} \quad (102)$$

As $\chi(\mathcal{T}_R^*) = 0$, we have $\chi(\mathcal{T}_R) > 0$, in both cases. Accounting for (99), we get

$$\begin{aligned} 0 < \chi(\mathcal{T}_R) &= e^{\text{EOS}}(\mathcal{T}_R, s_R) - \frac{p^{\text{EOS}}(\mathcal{T}_R, s_R)^2}{2a^2} - e^{\text{EOS}}(\mathcal{T}_R^*, s_R) + \frac{p^{\text{EOS}}(\mathcal{T}_R^*, s_R)^2}{2a^2} \\ &\quad + p^{\text{EOS}}(\mathcal{T}_R^*, s_R) \left(\mathcal{T}_R + \frac{p^{\text{EOS}}(\mathcal{T}_R, s_R)}{a^2} - \mathcal{T}_R^* - \frac{p^{\text{EOS}}(\mathcal{T}_R^*, s_R)}{a^2} \right) \\ &= e_R^* - \frac{(\Pi_R^*)^2}{2a^2} - e^{\text{EOS}}(\mathcal{T}_R^*, s_R) + \frac{p^{\text{EOS}}(\mathcal{T}_R^*, s_R)^2}{2a^2} + p^{\text{EOS}}(\mathcal{T}_R^*, s_R) \left(\frac{\Pi_R^*}{a^2} - \frac{p^{\text{EOS}}(\mathcal{T}_R^*, s_R)}{a^2} \right) \\ &= e_R^* - e^{\text{EOS}}(\mathcal{T}_R^*, s_R) - \frac{(p^{\text{EOS}}(\mathcal{T}_R^*, s_R) - \Pi_R^*)^2}{2a^2}. \end{aligned} \quad (103)$$

Similar lines can be used for $k = L$. \square

D All-regime approximate Riemann solver for the pressure subsystem

Following similar lines as in [27]: although the modified pressure scheme (32) is defined as a flux scheme, it is possible to find an approximate Riemann solver $(\mathbf{U}_{\text{RP}}^\theta, \Pi_{\text{RP}}^\theta, \mathcal{T}_{\text{RP}}^\theta)$ that enable to retrieve the numerical flux $\mathbf{P}_{j+1/2}^\theta$. We suppose that $(\mathbf{U}_{\text{RP}}^\theta, \Pi_{\text{RP}}^\theta, \mathcal{T}_{\text{RP}}^\theta)$ has the same structure as $(\mathbf{U}_{\text{RP}}, \Pi_{\text{RP}}, \mathcal{T}_{\text{RP}})$, we consider

$$(\mathbf{U}_{\text{RP}}^\theta, \Pi_{\text{RP}}^\theta, \mathcal{T}_{\text{RP}}^\theta, \phi_{\text{RP}}) \left(\frac{x - \bar{x}}{t}; \mathbf{U}_L, \Pi_L, \mathcal{T}_L, \phi_L, \mathbf{U}_R, \Pi_R, \mathcal{T}_R, \phi_R \right) = \begin{cases} (\mathbf{U}_L, \Pi_L, \mathcal{T}_L, \Phi_L), & \text{if } \frac{x - \bar{x}}{t} \leq -\frac{a}{\rho_L}, \\ (\mathbf{U}_L^{*,\theta}, \Pi_L^{*,\theta}, \mathcal{T}_L^{*,\theta}, \Phi_L), & \text{if } -\frac{a}{\rho_L} < \frac{x - \bar{x}}{t} \leq 0, \\ (\mathbf{U}_R^{*,\theta}, \Pi_R^{*,\theta}, \mathcal{T}_R^{*,\theta}, \Phi_R), & \text{if } 0 < \frac{x - \bar{x}}{t} \leq \frac{a}{\rho_R}, \\ (\mathbf{U}_R, \Pi_R, \mathcal{T}_R, \Phi_R), & \text{if } \frac{a}{\rho_R} < \frac{x - \bar{x}}{t}, \end{cases} \quad (104)$$

where Π_k, \mathcal{T}_k and Φ_k verify (85), $k = L, R$. The states $(\mathbf{U}_k^{*,\theta}, \Pi_k^{*,\theta}, \mathcal{T}_k^{*,\theta})$, $k = L, R$ are yet to be defined. First, we impose that $(\mathbf{U}_{\text{RP}}, \Pi_{\text{RP}}, \mathcal{T}_{\text{RP}})$ verifies the consistency in the integral sense

$$\begin{bmatrix} 2\mathbf{P}(\mathbf{U}_R) - 2\mathbf{P}(\mathbf{U}_L) \\ 2a^2(u_R - u_L) \\ -(2u_R - 2u_L) \end{bmatrix} = -\frac{2a}{\rho_L} \begin{bmatrix} \mathbf{U}_L^{*,\theta} - \mathbf{U}_L \\ (\rho\Pi)_L^{*,\theta} - (\rho\Pi)_L \\ (\rho\mathcal{T})_L^{*,\theta} - (\rho\mathcal{T})_L \end{bmatrix} + \frac{2a}{\rho_R} \begin{bmatrix} \mathbf{U}_R - \mathbf{U}_R^{*,\theta} \\ (\rho\Pi)_R - (\rho\Pi)_R^{*,\theta} \\ (\rho\mathcal{T})_R - (\rho\mathcal{T})_R^{*,\theta} \end{bmatrix} + \frac{\Delta x_L + \Delta x_R}{2} \begin{bmatrix} 2\{\mathbf{S}\} \\ 0 \\ 0 \end{bmatrix}. \quad (105)$$

We then enforce that the numerical flux resulting from (105) is \mathbf{P}_Δ^θ , which boils down to require that

$$\begin{bmatrix} 2\mathbf{P}_\Delta^\theta \\ 2a^2u_\Delta^\theta \\ -2u_\Delta^\theta \end{bmatrix} (\mathbf{U}_L, \Pi_L, \phi_L, \mathbf{U}_R, \Pi_R, \phi_R) = \begin{bmatrix} \mathbf{P}(\mathbf{U}_R, \Pi_R) + \mathbf{P}(\mathbf{U}_L, \Pi_L) \\ a^2u_R + a^2u_L \\ -(u_R + u_L) \end{bmatrix} - \frac{a}{\rho_L} \begin{bmatrix} \mathbf{U}_L^{*,\theta} - \mathbf{U}_L \\ (\rho\Pi)_L^{*,\theta} - (\rho\Pi)_L \\ (\rho\mathcal{T})_L^{*,\theta} - (\rho\mathcal{T})_L \end{bmatrix} - \frac{a}{\rho_R} \begin{bmatrix} \mathbf{U}_R - \mathbf{U}_R^{*,\theta} \\ (\rho\Pi)_R - (\rho\Pi)_R^{*,\theta} \\ (\rho\mathcal{T})_R - (\rho\mathcal{T})_R^{*,\theta} \end{bmatrix}. \quad (106)$$

Choosing $\rho_k^{*,\theta} = \rho_k$, $k = L, R$, relation (105) and (106) provide a linear system with respect to $u_k^{*,\theta}, \Pi_k^{*,\theta}, \mathcal{T}_k^{*,\theta}$ and $E_k^{*,\theta}$, $k = 1, 2$ whose solution is

$$\rho_L^* = \rho_L, \quad \rho_R^* = \rho_R, \quad (107a)$$

$$E_L^{*,\theta} = E_L^* - (1 - \theta) \frac{u_R - u_L}{2} u^*, \quad E_R^{*,\theta} = E_R^* + (1 - \theta) \frac{u_R - u_L}{2} u^*, \quad (107b)$$

$$u_L^{*,\theta} = u^* - (1 - \theta) \frac{u_R - u_L}{2}, \quad u_R^{*,\theta} = u^* + (1 - \theta) \frac{u_R - u_L}{2}, \quad (107c)$$

$$\Pi_L^{*,\theta} = \Pi_L^*, \quad \Pi_R^{*,\theta} = \Pi_R^*, \quad (107d)$$

$$\mathcal{T}_L^{*,\theta} = \mathcal{T}_L^*, \quad \mathcal{T}_R^{*,\theta} = \mathcal{T}_R^*. \quad (107e)$$

We now turn to positivity-preserving related properties. Let us note $e_k^{*,\theta} = E_k^{*,\theta} - u_k^{*,\theta 2}/2$, we have the following result.

Proposition D.1. Assuming again that a is large enough so that it satisfies the subcharacteristic conditions 38, we have

$$e_k^{*,\theta} - e^{EOS}(\mathcal{T}_k^{*,\theta}, s_k) - \frac{(p^{EOS}(\mathcal{T}_k^{*,\theta}, s_k) - \Pi_k^{*,\theta})^2}{2a^2} + \frac{(1-\theta)^2(u_R - u_L)^2}{8} \geq 0. \quad (108)$$

Proof. Let us consider the case $k = R$, by (107) we get

$$\begin{aligned} e_R^{*,\theta} - e_R^* &= E_R^{*,\theta} - E_R^* - \frac{1}{2}(u_R^{*,\theta^2} - u_R^{*2}) \\ &= (1-\theta)\frac{u_R - u_L}{2}u^* - \frac{1}{2}\left((u^*)^2 + u^*(1-\theta)(u_R - u_L) + (1-\theta)^2\frac{(u_R - u_L)^2}{4} - (u^*)^2\right) \\ &= -\frac{1}{8}(1-\theta)^2(u_R - u_L)^2. \end{aligned} \quad (109)$$

Using (100), we obtain

$$\begin{aligned} e_R^{*,\theta} - e^{EOS}(\mathcal{T}_R^{*,\theta}, s_R) &= e_R^{*,\theta} - e_R^* + e_R^* - e^{EOS}(\mathcal{T}_R^{*,\theta}, s_R) = -\frac{1}{8}(1-\theta)^2(u_R - u_L)^2 + e_R^* - e^{EOS}(\mathcal{T}_R^{*,\theta}, s_R) \\ &\geq -\frac{1}{8}(1-\theta)^2(u_R - u_L)^2 + \frac{(p^{EOS}(\mathcal{T}_k^{*,\theta}, s_k) - \Pi_k^{*,\theta})^2}{2a^2}. \end{aligned}$$

Similar lines can be used for the case $k = L$. \square

The relation (108) highlights the role of the inequality

$$\frac{1}{2a^2} \left(p^{EOS}(\mathcal{T}_k^{*,\theta}, s_k) - \Pi_k^* \right)^2 - \frac{(1-\theta)^2(u_R - u_L)^2}{8} \geq 0, \quad k = L, R \quad (110)$$

in obtaining stability properties for the modified scheme. We have the following proposition.

Proposition D.2. Let us note: $s_k^{*,\theta} = s^{EOS}(\mathcal{T}_k^{*,\theta}, e_k^{*,\theta})$, if (110) is satisfied, then

- the modified approximate Riemann solver (104) preserves the positivity of the internal energy, that is to say: $e_k^{*,\theta} > 0$, $k = R, L$,
- the modified approximate Riemann solver (104) verifies $s_k^{*,\theta} \geq s_k$, $k = R, L$,
- the modified approximate Riemann solver (104) is entropy satisfying in the sense that

$$-a(s_L^{*,\theta} - s_L) + a(s_R - s_R^{*,\theta}) \geq 0. \quad (111)$$

Proof. If (D.2) is satisfied, then $e_k^{*,\theta} \geq e^{EOS}(\mathcal{T}_k^{*,\theta}, s_k)$. By the assumption on the EOS, we have that $e_k^{*,\theta} > 0$. Now, considering a fixed $\bar{\mathcal{T}} > 0$, by (3) we know that $e' \mapsto s^{EOS}(\bar{\mathcal{T}}, e')$ is increasing, thus we deduce that $s^{EOS}(\mathcal{T}_k^{*,\theta}, e^{EOS}(\mathcal{T}_k^{*,\theta}, s_k^{*,\theta})) = s_k^{*,\theta} \geq s^{EOS}(\mathcal{T}_k^{*,\theta}, e^{EOS}(\mathcal{T}_k^{*,\theta}, s_k)) = s_k$, $k = L, R$. This implies (111). \square